Fascination of non-Newtonian fluids

R. A. Mashelkar

National Chemical Laboratory, Pune 411 008, India

Polymer solutions and melts, suspensions and many other structured fluids exhibit flow behaviour, that is rather bizarre and complex. The dramatic differences in the behaviour of normal fluids and such complex fluids are first described by examples. A continuum mechanics approach to formulate constitutive equations to explain this complex behaviour is presented. This is followed by a brief outline of the molecular modelling approach, both through the kinetic theory and the reptation models. Some illustrations on how and where such models can be used are given.

The complexities in handling the flows of non-Newtonian fluids have been explained by selecting three different areas. Instabilities in viscoelastic flows through contractions, particle motion in non-Newtonian fluids (including rapid external flows of viscoelastic materials) and stress-induced demixing have been chosen for this purpose. Some unresolved problems in non-Newtonian fluid mechanics have been highlighted. Directions for future research in this area have been also outlined.

Professor Travers was a great chemist and his contributions done in collaboration with Professor William Ramsay on the discovery and specification of inert gases are well known. Equally important were his contributions as the first Director of the Indian Institute of Science, since it was in that role that he laid a strong foundation for this great Institute.

In 1687 Isaac Newton wrote a simple equation defining the viscosity of a fluid as the coefficient of proportionality between the shear stress and the velocity gradient. Newton's equation does well while describing the flow of gases and liquids of low molecular weights such as air, water, hydrocarbons, etc. By the middle of the last century the mathematical description of the flow of such 'Newtonian' fluids was well established. This description is based on use of the laws of conservation of mass and momentum. However, Newton's equation cannot describe the flow of liquids containing polymers, especially when we deal with very large molecules, whose typical molecular weights may range from 10^5 to 10^8. The flow behaviour of these materials deviates significantly from a 'Newtonian' behaviour and hence they are called 'non-Newtonian' fluids.

Polymer fluid dynamics, which has to do with such non-Newtonian fluids, is a relatively new field; indeed the fluid dynamics of polymeric liquids has been studied only since about 1950. Authoritative monographs have appeared over the past few years in this field[1-4]. The rapid development of the plastics industry was a major incentive for the rapid growth of knowledge in this field.

Strange flows of non-Newtonian fluids

How do we know that Newton's law of viscosity is inadequate for polymeric liquids? There are many fascinating experiments that show that the flow of polymeric fluids is qualitatively different from that of Newtonian fluids. Figure 1 shows some of these experiments.

The behaviour of Newtonian and polymeric fluids near a rotating rod is compared in Figure 1 *a*. The surface of the Newtonian fluid is depressed near the rod, whereas the polymeric liquid tries to climb the rod. This climbing is known as the 'Weissenberg effect'.

In Figure 1 *b* a rotating disk placed at the surface of either fluid causes a primary flow in the tangential direction, but superposed on this primary flow is a secondary flow. Newtonian fluids are shoved outward by the rotating disk, move downward near the beaker wall and then move upward near the axis of the beaker. Polymeric liquids also have a secondary flow, but in the opposite direction.

Figure 1 *c* shows how fluids behave as they are pumped down a circular tube. We follow the motion by watching a streak of dye that is inserted before the motion starts; six successive snapshots of the streak are shown. When the pump is turned off at the fourth snapshot, the Newtonian fluid comes to rest, but the polymeric liquid 'recoils' as shown in the fifth and sixth snapshots. This illustrates the 'memory' of polymeric fluids. Because they do not return all the way to their initial configuration (as a rubber band would after

Based on the 'Morris Travers Memorial Lecture' delivered at the Indian Institute of Science, Bangalore, on 18 September 1992.

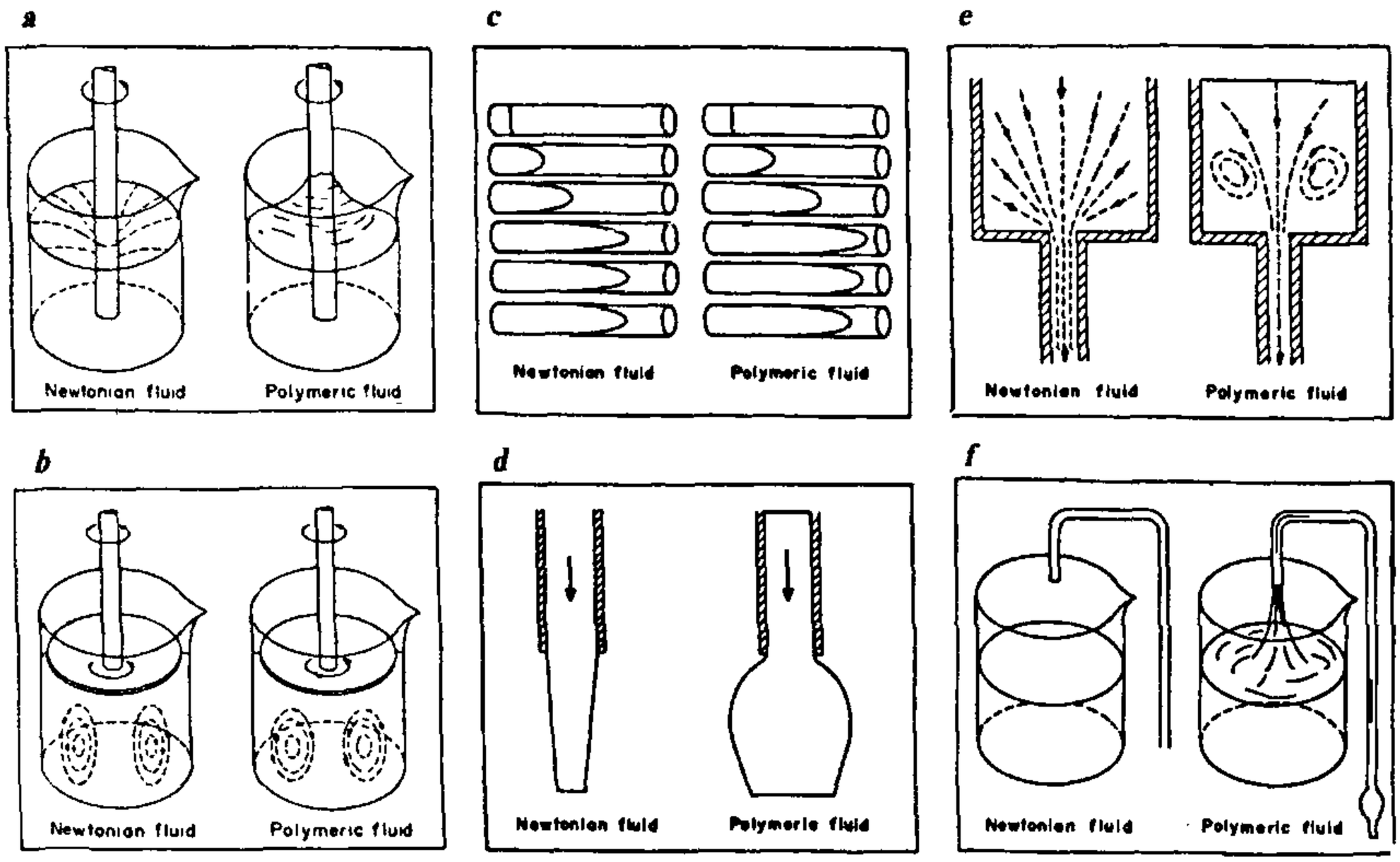

Figure 1. Complex flow behaviour of polymeric fluids.

being stretched), we say that these fluids have 'fading memory'.

Figure 1 *d* shows how a polymeric liquid swells when it emerges from a tube or slit. The cross-sectional area can increase by as much as a factor of five.

Figure 1 *e* shows how fluids flow from a large-diameter tube into a small-diameter tube in slow flow. In polymeric liquids, a vortex forms up-stream. Fluid particles trapped in this vortex do not move on into the small-diameter pipe.

Figure 1 *f* shows a siphon experiment. For Newtonian fluids, siphons work only as long as the upstream end of the tube is beneath the surface of the liquid. One can siphon polymeric fluids even if there is a gap of several centimeters between the surface of the liquid and the end of the tube.

In the experiments described above, the response of the polymeric liquid is qualitatively different from that of the Newtonian liquid. We are thus dealing with major variations in flow behaviour. We are faced with striking differences that can be explained only by rejecting Newton's law of viscosity and replacing it with some new and more general expression that can account for fading memory, recoil, and other bizarre phenomena we have seen. That is the challenge that the researchers involved in rheology and practitioners involved in dealing with these bizarre materials have faced over the years.

Let us first try to understand the striking differences in flow behaviour through simple physical arguments. Polymeric fluids respond to deformation depending upon the characteristic time-scale of the fluid, say, a relaxation time. For fluids such as water, the relaxation time-scales are of the order of 10^{-13} s. For solutions or melts of high-molecular-weight polymers, the time constants could range from seconds to minutes. The ratio of the relaxation time of the fluid to a characteristic time of the process is termed as the Deborah number. This Deborah number plays a crucial role in determining the response of the material. The formalization of fluid classification is shown in Figure 2. We can see that depending upon the region of operation, the material response can differ dramatically. The same fluid at low Deborah numbers can behave as a Newtonian fluid whereas at high Deborah numbers, it can behave like an elastic solid. In labelling the material as a fluid or a solid, the Deborah number and the magnitude of strain need to be defined carefully. This can be illustrated with a simple example. A silicon putty left on the table will flow as a fluid if sufficient time is allowed. Here under low strain-low Deborah number conditions, the flow occurs as if it was a fluid. On the other hand, the same silicon putty can be bounced practically like a rubber ball on the table. Here the relaxation time of the silicon putty remains the same but the time-scale at which the experiment is

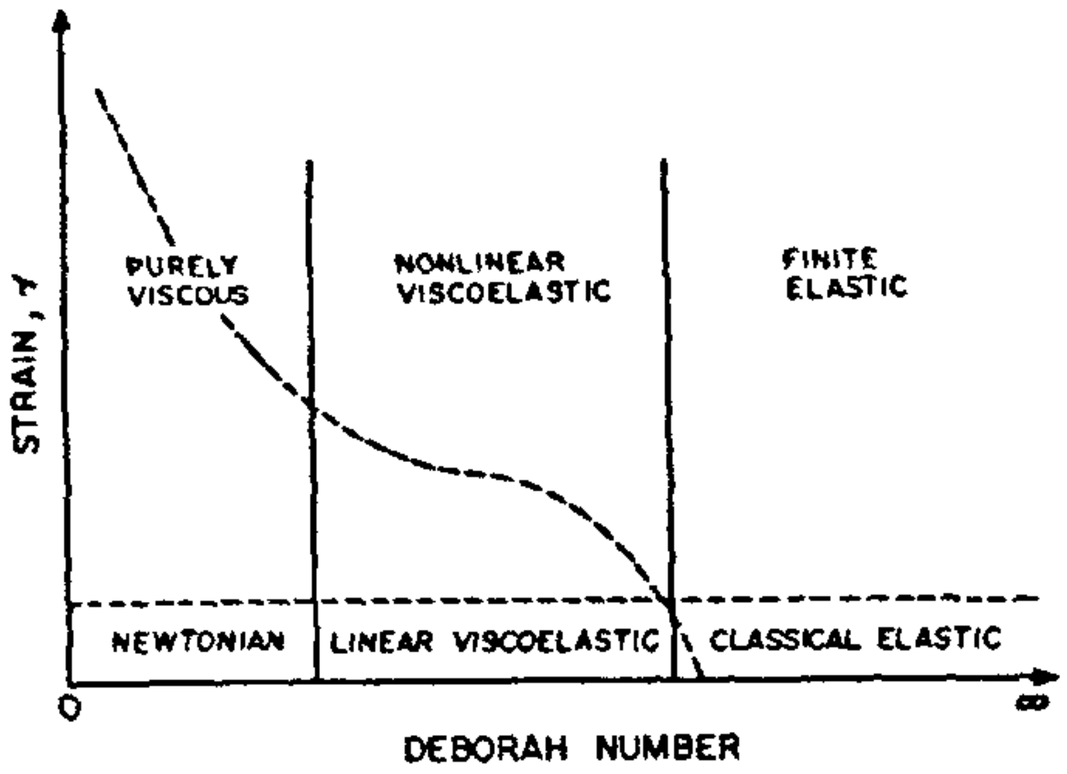

Figure 2. A classification of fluid behaviour in the strain-Deborah number domain.

performed is of the same order as the relaxation time and large Deborah numbers arise. This gives rise to a solid-like response. As we shall show later on, such dimensionless numbers play a key role in engineering analysis of non-Newtonian flows[5,6].

Polymeric fluids are also 'memory fluids'. A fluid like water has practically no memory. It assumes the shape of the container. An elastic solid has a perfect memory. A rubber band that is stretched gets back to its original position when the strain is released. Intermediate is the behaviour of a polymer fluid. Fortunately the fluids have a 'fading memory'. Just as a human being remembers what happened to him in the recent past better than what happened to him in the distant past, similarly the material remembers the recent history of strains and stresses more than it does the history in the distant past.

All this physical description sounds interesting but how does one formalize this in mathematical terms? This has been the vexing problem that has been faced by fluid mechanicists and rheologists over the last few decades. Over the past forty years, strategies for handling such problems have been worked out. Let us review some of these.

Strategy for solution of non-Newtonian flow problems

In order to solve flow problems in polymer fluid dynamics it is necessary to have a constitutive equation that gives the stress tensor in terms of various kinematic tensors. This central problem can be partially solved by three different approaches:

The first approach is to use the experimental measurements of rheological properties. These are certainly helpful, since the experimental data can be used to construct empirical constitutive equations that reproduce the measured quantities within reasonable limits. This approach has its own limitation, since in any one rheometric experiment usually only one or two combinations of stress tensor components can be measured.

The second approach is to use continuum mechanics. This can supply information about constitutive relations in the form of various types of ordered expansions that follow from some general postulates about the stress tensor. However, fluid dynamicists find expressions obtained in this way to be of limited value, because their use is restricted to a rather small range of the kinematical variables.

Thirdly, molecular theories can be used to obtain rheological properties, and in some cases, complete constitutive equations, in terms of the parameters that characterize the mechanical model that purports to describe the most important features of the polymer molecule. Here again, there is a limitation. The extent to which the kinetic theory can describe the polymer liquid response depends on how realistic the mechanical model is, but an increase in the reliability of the model and its closeness to realism is accompanied by a formidable increase in the mathematical and computational complexity.

A combination of the three approaches above is what is used today. Molecular models and kinetic theory suggest forms for constitutive equations that hold out the promise of being useful over wide ranges of kinematic variables. In obtaining the constitutive equations one makes use of continuum mechanics relations involving various strain and rate-of-strain tensors. The parameters in the final constitutive equation cannot be computed a priori. Therefore, they are evaluated by comparing the computed rheological properties with those obtained from experiments. We will give below the essence of these individual approaches rather briefly.

A continuum mechanics approach

The description of a Newtonian fluid such as air or water is simply given by

$$\tau = \eta D \tag{1}$$

where τ is the stress tensor, D the rate of deformation tensor and η the viscosity.

However, for a non-Newtonian fluid a very complex description is required. An interesting approach is that of the 'simple fluid' developed by Noll[7]. He enunciated four major principles including determinism of stress, local action, non-existence of a natural state and the fading memory. The general mathematical description

of 'simple fluid' requires that the stress in some functional over the past history of the deformation is represented by

$$\tau = H_{s=-\infty}^{s=0} \text{ (strain)} \tag{2}$$

Limiting cases of equation (2) can be derived leading to meaningful modelling of real fluid behaviour. For instance, if the motion is slow (in the sense that the changes in deformation occur slower than some natural time-scale for the fluid) then the simple fluid reduces to the fluid of grade n.

$$\sigma = -pI + \tau = \sum_{n=0}^{N} \sigma_n, \tag{3}$$

where σ is the total stress, τ the deviatoric stress, p the isotropic pressure and I the unit tensor. For a fluid of grade 2, we get

$$\tau = \alpha_1 A^{(1)} + \alpha_2 (A^{(2)})^2 + \alpha_3 A^{(2)} \tag{4}$$

where $A^{(1)}$ and $A^{(2)}$ are the Rivlin–Erickson deformation rate tensors and α_1, α_2 and α_3 are material parameters.

Such a fluid has a constant shear viscosity as given by:

$$\eta(\dot{\gamma}) = \alpha_1, \tag{5}$$

and demonstrates the effect of fluid elasticity through a non-zero normal stress differences in shear flow given by:

$$\tau_{11} - \tau_{22} = 2\alpha_3 \dot{\gamma}^2 \tag{6}$$

$$\tau_{22} - \tau_{33} = -(2\alpha_3 + \alpha_2)\dot{\gamma}^2. \tag{7}$$

While such a 'slow flow' approximation is useful, transient behaviour is not readily predicted. Green and Tobolsky[8] developed integral expansions which were later formalized in a single integral form by Lodge[9] as a rubber-liquid. This development led to

$$\tau = \int_{-\infty}^{t} N(t-t') C^{-1}(t,t') \mathrm{d}t', \tag{8}$$

where $N(t-t')$ is the memory function for the fading memory and C^{-1} is the Finger stress tensor. The memory function could be expressed either in a discrete form

$$N(t-t') = \sum_{n=1}^{N} \frac{G_n}{t_n} \exp\left(-\frac{(t-t')}{\lambda}\right) \tag{9}$$

or in a continuous form

$$N(t-t') = \int_{-\infty}^{\infty} H(\lambda) \exp\left(-\frac{(t-t')}{\lambda}\right) \mathrm{d} \ln \lambda \tag{10}$$

where λ is the characteristic time for the fluid and $H(\lambda)$ represents a relaxation time spectrum. Note the negative exponentials in equations (9) and (10), which appropriately assign larger importance to events in the recent past than they do to the events in the distant past.

The rubber-like fluid with minor modifications helps us in developing several constitutive relations. The memory function can be modified so that it becomes a function of the state of deformation and leads naturally to nonlinear viscoelastic response. The rubber-like liquid is qualitatively correct at slow deformation rates and the extension of Lodge's concept by changing the memory function provides a basis for improving the constitutive relationship and enables the prediction of practically observable nonlinear viscoelastic response. Many efforts in the past to achieve this goal have been done by using rate-dependent memory, strain-dependent memory, stress-dependent memory, etc.

The first models of viscoelasticity derived their origin from mechanical analogues and were expressed in the form of rate equations. The Maxwell model formulation, for instance, naturally results out of a superimposition of an elastic response over a Newtonian one as given by:

$$\tau + \frac{\delta \tau}{\delta t} = \eta D, \tag{11}$$

where $\delta\tau/\delta t$ is some properly-defined tensor derivative of stress such as the Jaumann or Corotational derivative, and D is the rate of deformation tensor.

Polymer dynamics through molecular modelling

Polymers are molecules of very large molecular weight, and there is an enormous variety in their chemical architecture. Polymers are formed by stringing together certain repeating groups of atoms in such a way that an extremely long chain is formed. Such a chain can be oriented in space. In addition, it has a lot of flexibility resulting from the large number of internal degrees of freedom. The chain can appear in a coiled-up configuration, or it can be stretched out into a long string-like configuration.

To study the kinetic theory of polymeric liquids, one has to select some kind of mechanical model that represents the actual polymer molecule. Flory[10], in his study of the configurations of polymer molecules in systems at equilibrium, actually used rather detailed

models that account for chemical bond lengths, bond angles and rotational isomeric states. However, such a realistic molecular modelling is not possible today in rheological studies, because the motion of molecules in flowing systems is so much more complicated than that in equilibrium systems.

In *molecular modelling*, the a priori assumptions are more physical than mathematical. On the basis of known information on the gross structural features of the polymeric chain (e.g. linear and flexible, star-like and flexible, rigid rod-like, etc.) and by using general concepts of statistical mechanics, the basic steps in establishing a molecular model are as follows[11]:

(i) The polymeric molecule is represented as a mechanical object endowed with those 'molecular' properties which are thought to be relevant. Thus the object will be made up of a certain number of friction points, entropic springs, rigid segments, etc., depending on the specific polymer (see Figure 3). The advantage of substituting for the real chain such as artificial object consists in the fact that *the configuration in space* of the latter can be specified with a simpler, usually smaller set of coordinates than the polymer molecule itself.

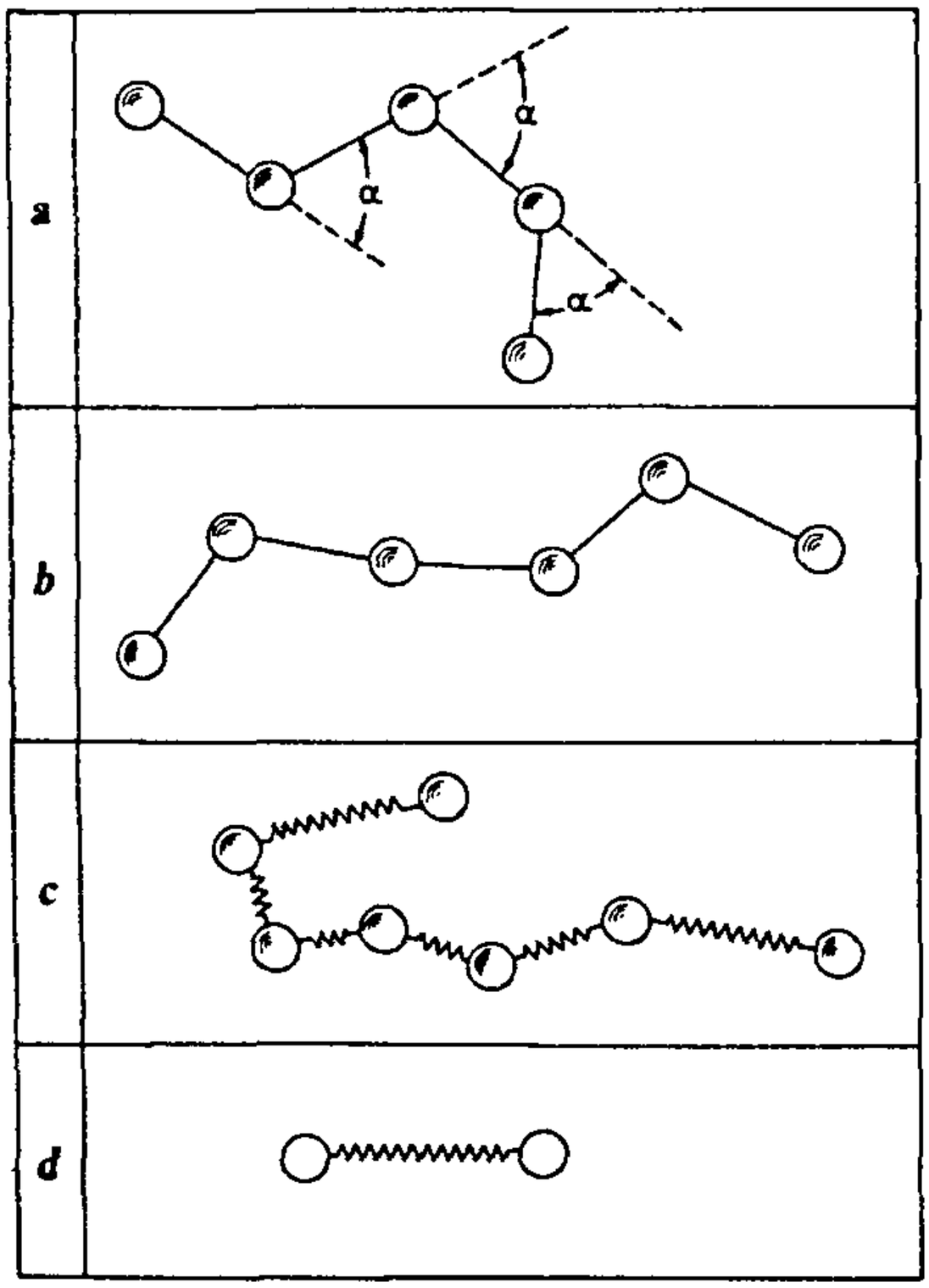

Figure 3. Mechanical models representing chain-like polymer molecules in kinetic theory: *a*, Kirkwood–Riseman chain; *b*, Kramers chain; *c*, Rouse–Zimm model; *d*, elastic dumb-bell model.

(ii) Since the molecules are subject to random thermal forces, it is of course meaningless to speak of the effects induced by the motion of the liquid on the configuration of any one of them. Rather, one is interested in the effects induced upon the *distribution* of configurations. Thus, the second step in the analysis consists of writing down the *equation of change* of the distribution function. This usually involves simple concepts of continuity and force balance.

(iii) The third step establishes which average, involving the configuration coordinates, must be made to obtain the stress tensor (or the optical tensor, if birefringence is investigated).

The three steps above define the essence of the molecular model. The predictions of the model for a given flow are found, by solving the equation of the distribution as written in step (ii) and then using this distribution to perform the average of step (iii). In some favourable cases, the solution procedure can be simplified by avoiding the explicit determination of the distribution function. The equation of change of the distribution is manipulated so as to become the *equation of change for the average which provides the* stress tensor. If this can be done for an arbitrary flow, the stress constitutive equation is obtained explicitly. In other cases, only certain predictions can be readily derived whereas others are obtained through painstaking numerical procedures or, possibly with the help of additional simplifying assumptions.

The advantage of this approach is obvious, since it allows one to relate the predicted features of macroscopic behaviour directly to molecular properties via the model representation. Depending on the agreement with the experimental results, it is always possible, at least in principle, to introduce in the model physically significant corrections so as to approach progressively a satisfactory representation. Conversely, if the quest is for a mathematically more tractable, simplified model, refinements can be dropped, knowing beforehand which physical effects are being left out.

More quantitative insight into kinetic theory

Some insight into the quantitative approach in molecular modelling through a kinetic theory approach[1] can be now considered. The stress tensor τ describes the force transmitted across an arbitrary mathematical plane moving with the fluid (the force per unit area from the negative side to the positive side across a plane with unit normal vector $\mathbf{n}$ is just $\mathbf{n}.\tau$). There are five mechanisms contributing to the force (see Figure 4)

- the momentum transfer as the solvent or polymer 'beads' cross the surface (τ_K)

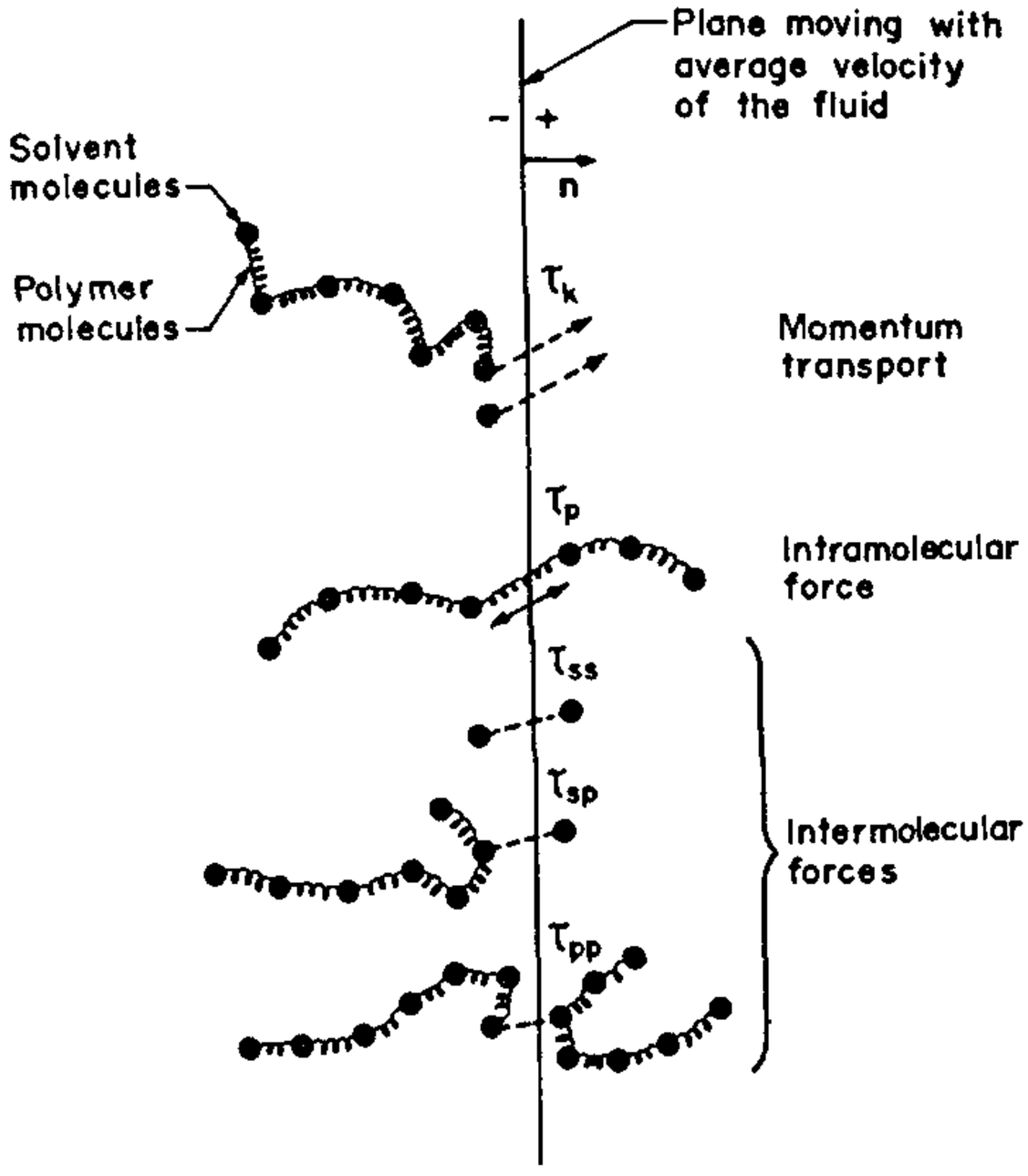

Figure 4. Molecular mechanisms that contribute to the stresses in a polymeric liquid.

- the tension in a polymer molecule that straddles the surface (τ_p)
- the force between two solvent molecules on opposite sides of the surface (τ_{ss})
- the force between a solvent molecule and a polymer molecule (τ_{sp})
- the force between two polymer molecules (τ_{pp}).

Hence the total expression for the stress tensor is

$$\tau = \tau_K + \tau_p + \tau_{ss} + \tau_{sp} + \tau_{pp}. \tag{12}$$

The expression for τ_p involves the contribution of intramolecular forces. Here one must average over all possible configurations of the macromolecule in the particular flow system being studied, that is, one has to know the 'configurational distribution function' Ψ. This defines the probability of each of the very numerous configurations of the polymer chain. Similarly, to calculate the kinetic contribution (τ_K), knowledge of the velocity distribution of the beads is needed. To get the intermolecular force contributions τ_{ss}, τ_{sp} and τ_{pp}, one needs the various pair distribution functions. It is difficult to obtain these last two distribution functions, so one proceeds by making some assumptions.

We can write down an equation of continuity for the distribution function $\Psi(r_1, r_2, \cdots, r_N, t)$, which gives the probability that the polymer molecule finds itself in the configuration $r_1, r_2, \cdots, r_N$ at time t:

$$\frac{\partial \Psi}{\partial t} = -\sum_{v=1}^{N} \left(\frac{\partial}{\partial \mathbf{r}_v} \cdot \dot{\mathbf{r}}_v \Psi \right).$$

Here $\mathbf{r}_v$ is the position of the vth bead and $\dot{\mathbf{r}}_v$ is its velocity. This equation simply states that when a polymer molecule leaves one configuration it must turn up in another. This equation by itself is of little interest. What we need is an expression for the bead velocity $\dot{\mathbf{r}}_v$. This is obtained by writing down an equation of motion for each of the N beads of the bead-spring model:

$$m_v \ddot{\mathbf{r}}_v = \mathbf{F}_v^{(h)} + \mathbf{F}_v^{(Br)} + \mathbf{F}_v^{(\varphi)}$$

$$v = 1, 2, \cdots, N. \tag{14}$$

Equation (14) implies that the product of bead mass and bead acceleration is equal to the sum of the various forces acting on a bead namely the hydrodynamic drag force, the Brownian motion force and the spring force associated with the intramolecular potential. One usually omits the acceleration terms on the left side of the equation so that the equation represents just a balance of forces. After one introduces specific expression for the various forces (including a form of Stokes' law for the hydrodynamic drag, which involves the bead velocity $\dot{\mathbf{r}}_v$), one can solve equation (14) for the bead velocity and substitute the result into equation (13) to obtain a second-order partial differential equation for Ψ.

Several mechanical models have been used for the description of kinetic theory of flexible, chain-like polymers. Some of these are shown in Figure 3. ***a*** The Kirkwood–Riseman freely rotating chain is made up of 'beads' joined together by massless 'rods', but the angles between successive rods are fixed; ***b*** the Kramers freely jointed chain is composed of beads joined by rods, with universal joints at the beads; ***c*** the Rouse–Zimm chain is constructed from beads and 'springs', with universal joints; and ***d*** the elastic dumb-bell is made up of just two beads and spring. These models have been listed in decreasing order of complexity, but each model is supposed to represent long-extensible molecules that can undergo rotational and uncoiling motions. The constant angles between the rods in the Kirkwood-Riseman chain describes the inherent stiffness in polymer chains, which the other models do not describe. The elastic dumb-bell model clearly is incapable of mimicking the responses associated with the many internal degrees of freedom of a polymer molecule. Its simplicity however, has made it quite useful as a tool in understanding of the relation between molecular motions and rheological phenomena.

The choice of molecular model will generally depend on the contemplated use of the kinetic theory results. To describe the small-amplitude oscillatory experiment used for studying linear viscoelastic responses, one needs a model with many internal degrees of freedom, particularly if it is desired to describe effects at high frequencies; the Rouse-Zimm chain model has proven to be quite useful in this instance. To describe the steady-state shear flow experiment, where the overall rotation of the molecule is the principal molecular motion involved, it is not particularly necessary to use a model with many beads since the small scale motions are not activated in the flow. To describe an elongational flow experiment, in which the molecules are being stretched out considerably, a model that has a finite extensibility is required, such as the Kramers chain or an elastic dumb-bell with a nonlinear spring that can be stretched only to a finite limit. If one wishes to be able to describe all three of these types of experiments quantitatively, then a more comprehensive model such as the Kirkwood–Riseman chain has to be used, since it can describe chain orientation, small-scale motions, finite extensibility, and chain stiffness.

The various models contain a number of constants, such as the number of beads, the spring constants and the length of rods. These are, of course, empirical parameters, and are not unlike the constants in the Lennard–Jones potential used widely in the statistical mechanics of gases. In many instances one can eliminate these parameters in favour of more fundamental molecular constants or parameters derived experimentally from bulk properties.

Rheology of dilute vs concentrated systems

Flows of dilute or of concentrated solutions and melts of flexible polymer molecules need to be treated separately. The term 'dilute' means that the molecules have minimal overlap with each other. Concentrated solutions have considerable molecular overlap. The rheology of concentrated solutions is similar to that of bulk polymer melts. We must distinguish between dilute solutions and concentrated solutions or melts, because there are major differences in the rheology of fluids in these two categories.

In a dilute solution, the interactions among polymer molecules can be ignored by definition. Thus, the corresponding molecular models only account for the intrinsic properties of the macro-molecules themselves, in conjunction with their dynamic interactions with the solvent. The effect of the latter is simply that of a viscous continuum in which the polymeric chains are immersed. Conversely, in concentrated solutions and melts, the interactions between the chains is expected to play a major role. These concentrated systems show a more complex behaviour.

Polymer melts behave in two different ways, depending on molecular weight. It is well known that the viscosity is proportional to M, if M is smaller than a critical value M_c (of order 10^4 for most polymers). It, however, becomes proportional to $M^{3.4}$, if $M > M_c$ (ref. 10). More generally, it was found that the observed behaviour for $M < M_c$ closely follows the predictions of the Rouse model. Since this model had originally been conceived for dilute solutions, the observed agreement for polymer melts was somewhat surprising. The explanation was given on the basis that the dynamic interaction between any chain and the surrounding chains could still be modelled as if the medium was a viscous continuum, i.e. no special effects due to the polymeric nature of the surrounding molecules come into play when $M < M_c$. By implication, it was inferred that the non-Rousean behaviour which is observed for $M > M_c$ was due to a peculiar effect of very long molecules being in close contact to one another. It was assumed that long chains form entanglements. Though they were not defined in any precise way, the *entanglements* were clearly related to the obvious impossibility for the chains to cross each other by cutting through their backbones.

Unfortunately, this appealingly simple concept was not adequately developed for a long time. Two different ways of treating entangled systems were commonly used. In one of them, the entanglements are modelled as if they were additional friction points along the chain. The model is thus essentially that of Rouse, the extra friction being used to explain the viscosity increase above that predicted by the original Rouse theory. Apart from the arbitrariness of this ad hoc adjustment, the modified Rouse models proved unable to predict correctly the other features of the viscoelastic behaviour.

A second group of models approached the problem from an entirely different viewpoint. It was well known that rubbers are networks made up of chemically cross-linked polymeric chains. The rubber elasticity theory had been developed since the early forties and showed a substantial agreement with experimental observations. By an extension of this idea, concentrated polymeric liquids were modelled as 'networked' liquids, where the entanglements played the role of temporary cross-links. Impermanent junction network theories were advanced as early as 1946 by Green and Tobolsky[8] and, more systematically, by Lodge[9], and further developed up to recent times. We have already made a reference to such developments earlier (see, e.g., equation 8). An inevitable shortcoming in this approach is that the basic elements of a network model are the network strands, i.e. the chains which run from a junction to the next one. In a chemically cross-linked network, the mechanical behaviour is indeed essentially determined by these well-defined chains. In an impermanent

network, however, the rates of the junction destruction and reformation processes also play a crucial role, in so far as they determine the liquid-like character of the material. Now, in the impermanent network idea *per se* there is no quantitative suggestion about these rates. They must be assumed a priori in an esentially arbitrary way. In other words, the concept of an impermanent network made up of entangled chains, though intuitively appealing, is ultimately not very informative. In shifting the emphasis from the primary polymer chains to the network strands, the model becomes incapable of predicting the dependence of properties on the molecular weight of primary chains. By analogy with the case of cross-linked rubbers, one might have hoped that the network idea would provide at least a good description of the 'elastic response' of entangled liquids. Even this expectation was fulfilled only in a few limiting conditions.

A fresh approach to the modelling of long chains in dense systems started developing in the late sixties, rapidly gaining momentum in recent years. This fundamental progress is due to S. F. Edwards, P. G. de Gennes and M. Doi. The seminal contributions of these authors have been summarized in elegant monographs[12,13]. Let us look at these contributions somewhat more closely.

Reptation model

The essence of this model is based on the fact that one can trace the 'viscoelastic' behaviour to the knotting of the chains of monomers that make up the polymers. Shearing forces tend to undo certain knots, but this takes a finite time τ_r. In a time greater than τ_r the original knots fade out, and the melt flows. Over shorter times the original knots are all present, and the melt behaves like an elastic network.

A major problem is to transform these qualitative ideas into a theory. An obvious way to proceed is to have a detailed analysis of knot structures and knot statistics. This approach had limited success due to several reasons. To define topologically a knot between two curves, each curve must be closed. However, the essential behaviour of chains at times close to τ_r depends crucially on the fact that they are open, and can modify their knots. The theory of knots, unfortunately, is far from complete. Mathematicians know explicitly only a few topological invariants characterizing knots. de Gennes'[12] approach was to concentrate on individual polymer chains as they move in the complex polymer melt by 'reptation' (from the Latin reptare, to creep), much as snakes would move through a set of fixed obstacles. The essence of the approach can be simply explained.

Edwards[14] clearly stated that the effect to be examined in entangled systems was the reduced number of configurations available to the chain, which are 'boxed in' by other chains. Figure 5*a* shows schematically a segment of a long chain together with the obstacles formed by other chains depicted as dots. The chain cannot pass these dots, since in a real system it will mean cutting through the backbone of other chains, which is clearly not possible. Figure 5*b* shows two more permissible combinations of the same chain. One of them, shown as a broken line, is very special. It is obtained by imagining that the chain is pulled taut. Later on Edwards called this unique configuration the 'primitive path' of the chain or, alternatively, the 'primitive chain'. Although the specific statistics of this situation is unknown, we propose intuitively that configurations beyond a certain distance from the primitive path are unlikely. We thus imagine that a tube-like region exists, around the curvilinear axis formed by the primitive path, to which the chain is effectively confined. This tube, shown in Figure 5*c*, represents the 'boxing in' effect in entangled system as proposed by Edwards. Although the tube diameter is not coincident with the obstacle mesh size, a close relationship between them exists. We also envisage that

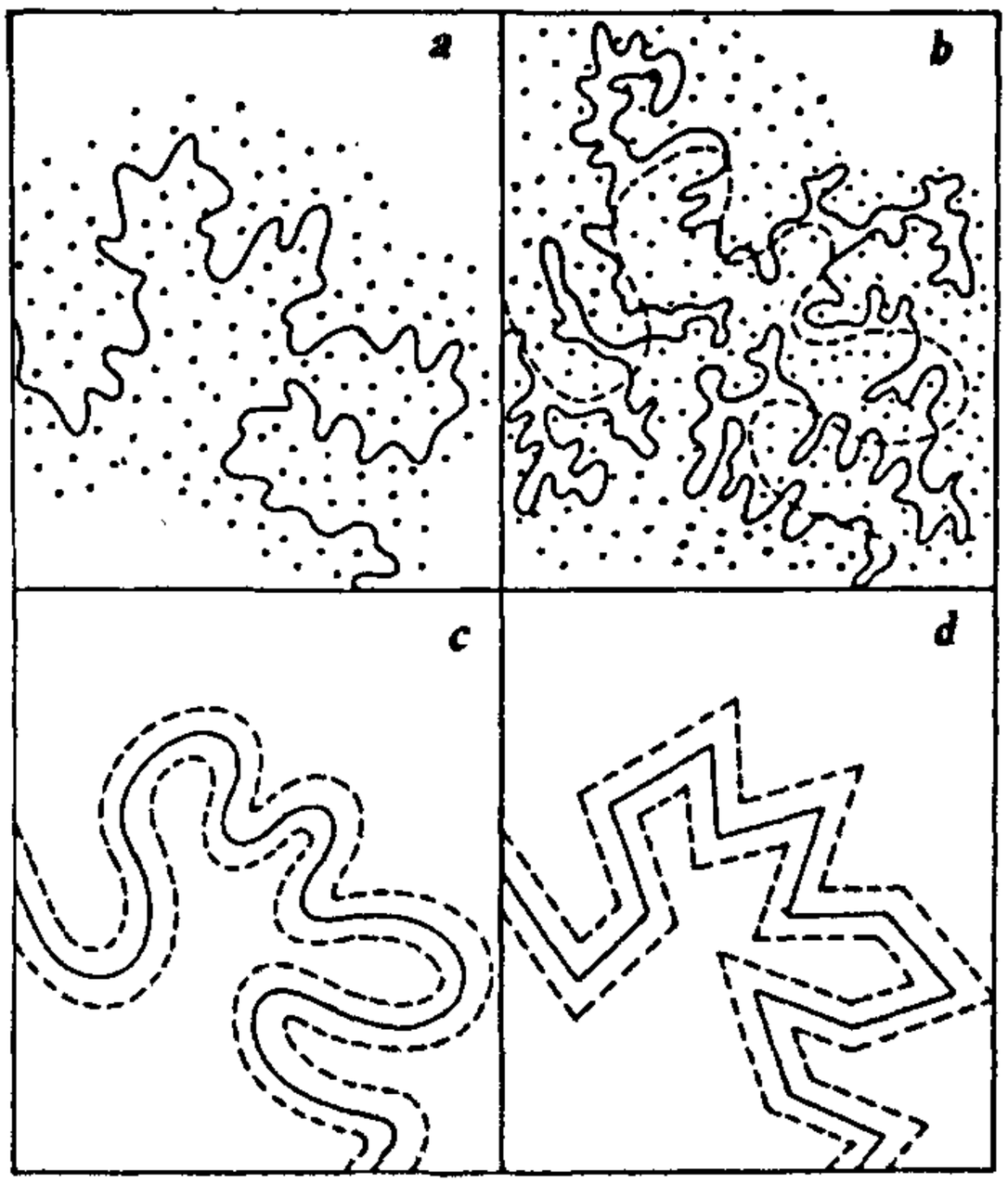

Figure 5. Representation of entangled systems. *a*, The chain surrounded by obstacles. *b*, The primitive path of the chain (broken line) and an improbable chain configuration (full line). *c*, The curvilinear tube simulating the obstacles. The axis of the tube is the primitive path. *d*, Tube and primitive path in the discretised form of a random walk.

if the chains are very long, the mesh size is independent of the chain length, the chain ends being very dilute in the system.

A polymer melt at a given temperature has a measurable characteristic frequency $1/\tau_r$ separating the viscous domain from the elastic domain. The time τ_r is extremely sensitive to the length of the polymer chains in the melt. This length can be specified in terms of the number N of monomers in the chain. We then find

$$\tau_r = \tau_0 N^{\alpha}, \tag{15}$$

where τ_0 is a microscopic time on the order of 10^{-10} s in melts, and experimental values of the exponent α are about 3.4. Amazingly enough, based on the idea of reptation, a straightforward argument gives $\alpha = 3$, which is quite close to the exponent 3.4 obtained experimentally.

Consider time intervals that are comparable to τ_r. For such long intervals one can ignore the details of the test chain's 'reptation' and take a macroscopic point of view, in which the test chain moves as a whole like a wet rope in a pipe. One essential parameter is then the chain's 'tube mobility' μ_{tube}, defined as v/f, where v is the velocity with which the chain moves along the tube when it is pulled by a force f. This mobility is inversely proportional to the chain's length, for which N is the measure.

Using Einstein equation for diffusivity, we can calculate the chain's Brownian motion along the tube.

$$D_{tube} = kT\mu_{tube} \tag{16}$$

Thus, the diffusivity is also inversely proportional to the chain length N. Along a fixed tube, then, a polymer chain's mean square displacement $s^2(t)$ due to Brownian motion has the standard form

$$s^2(t) = 2D_{tube}\, t. \tag{17}$$

We are now fully equipped to understand the nature of the relaxation time τ_r. Figure 6 illustrates the basic process of relaxation, in which the chain generates new tube portions at random as it advances. The original tube is completely wiped out after a time τ_r for which $s(r)$ is comparable to the original tube length L. Thus

$$\tau_r \approx L^2/D_{tube} \sim N^3. \tag{18}$$

Here we have used the fact that L is linear in N while D_{tube} is inversely proportional to N. The proportionality of the relaxation time to the cube of the chain length is the fundamental result of the reptation model.

These ideas led Doi and Edwards[13] to develop a precise theory of viscoelastic effects in melts. For small perturbations, that is, for linear viscoelasticity, their

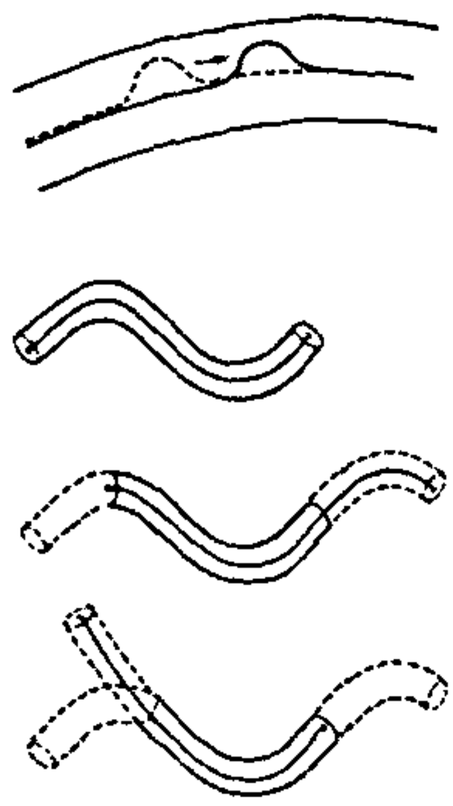

Figure 6. Snake-like motion and diffusion of a 'test chain'.

major result is the detailed form of the 'memory function', which gives the stress at time t as a function of the strain rates at earlier times t. It turns out that the memory function $M(t-t')$ is exactly proportional to the 'tube memory' that the sequence of sketches in Figure 6 illustrates. The average fraction of the chain length that, at time t, is still trapped in the tube that was defined at time t'. Computations of this fraction show that it decreases exponentially at large times

$$M(t) \to \exp(-t/\tau_r).$$

More generally, the Doi-Edwards analysis appears to give a good description of the rheology of entangled polymers provided that the distribution of polymer chain lengths N is narrow and the molecular weight is high enough that the macroscopic description given in the foregoing is valid.

Engineering analysis

It is useful to pause briefly, and recapitulate some important aspects of polymer rheology, since a frequent reference to some of these will be made later on. Some of the material parameters of non-Newtonian fluids will assume importance in our subsequent discussion. These pertain to the first and second normal stress difference and the apparent viscosity. It is useful to recall that the first normal stress difference, $N_1 \equiv \tau_{11} - \tau_{22}$, and the second normal stress difference, $N_2 \equiv \tau_{22} - \tau_{33}$, are zero for a Newtonian fluid. Further, apparent viscosity $\tau_{12}/\dot{\gamma} (= \eta)$ is a constant, where $\dot{\gamma}$ is the shear rate. Both dilute solutions and melts of polymers, however, can possess first normal stress differences of significant magnitude. While dilute solutions show little shear

thinning, the shear viscosity of concentrated solutions or melts can decrease by several orders of magnitude as the shear rate increases. Also, in concentrated solutions and melts, the first normal stress coefficient, $\Psi_1 \equiv N_1/\dot{\gamma}^2$, which is a constant $\Psi_{1,0}$ at low shear rates, can decrease by several orders of magnitude as γ increases. This decrease in Ψ_1 is another manifestation of shear thinning. In addition, melts and concentrated solutions in shearing flows often have a significant negative second normal stress coefficient, $\Psi_2 \equiv N_1/\gamma^2$, while in dilute solutions this quantity can be nearly zero.

All constitutive equations for viscoelastic fluids require the specification of at least two material parameters, namely, the zero shear viscosity η_0 and at least one relaxation time λ. For dilute and concentrated solutions or melts, these parameters can be estimated theoretically if one knows the molecular weight of the polymer and the solvent viscosity. In a dilute solution, the longest relaxation time depends on the chemical nature of the polymer, on the solvent viscosity, and on the molecular weight of the polymer molecule in the following way[4].

$$\frac{\lambda}{\eta_0} = \frac{2K M^{1+a}}{RT}, \tag{19}$$

where, R is the gas constant and T the absolute temperature. The exponent α for a flexible polymer is usually between 0.5 and 0.8, depending on the degree to which the solvent tends to swell the polymer. A theta solvent by definition has no swelling tendency, and $\alpha = 0.5$. The parameter K reflects the frictional properties of the polymer and the solvent swelling characteristics.

For concentrated solutions or melts, the scaling of the zero shear viscosity and the relaxation time is non-trivial, but can crudely be approximated from the data of Osaki *et al.*[15] as

$$\frac{\lambda}{\eta_0} = \frac{K^3 M^{3/2}}{10^6 f^3}, \tag{20}$$

where $f = c/c^*$, c^* being the concentration at which the polymer molecules begin to overlap appreciably. The solution is only weakly entangled unless f is 10 or greater.

The parameter λ will be used in defining dimensionless numbers. One important dimensionless number is the Weissenberg number ($Wi = \lambda V/d$). Here, V is a characteristic velocity and d is the small dimension of the flow geometry so that V/d is a characteristic velocity gradient. Flow time can be either the residence time of a fluid particle in the flow, or the characteristic time of a flow transient, such as the time over which a fluid particle in the flow, or the characteristic time of a flow transient, such as the time over which a fluid particle experiences a changing velocity gradient as it passes through a diameter contraction in pipe. Sometimes, flow time is defined for steady rotational flows as the reciprocal of the angular velocity ω of the rotating surface; in that case, $De \equiv \lambda\omega$. These dimensionless numbers play a crucial role in the design and analysis of situations involving non-Newtonian flows (see e.g., equations (5), (6)).

Some special problems

In the foregoing, we have provided a background on the basic rheological behaviour of non-Newtonian fluids and also shown an approach to model these fluids. As engineers, we will be concerned with the use of such knowledge in solving problems of pragmatic importance. What I would like to focus on are three different problems, which demonstrate the extent of understanding that we have today and how exactly it has been used in problem solving.

The first problem concerns instabilities in polymer processing. Even simple extrusion of a molten polymer to get a solid polymeric rod may pose formidable difficulties depending upon the rheological complexities. Many interesting aspects of this important problem will be highlighted by considering the special problems linked to flows with restrictions and then the problem of extrudate distortions and fractures arising out of instabilities.

The second problem area will be concerned with the motion of non-Newtonian fluids past submerged object, such as spheres, cylinders etc. The objective here is to show the dramatic differences that exist between motion in Newtonian fluids and that in non-Newtonian fluids.

The third problem area will be concerned with the behaviour of polymer solutions in non-homogeneous deformation fields. The implications of demixing of polymer solutions under stress are rather profound. The phenomena range from formation of slip layers at solid surfaces to stress-induced phase changes such as polymer precipitation on deforming a polymer solution or a melt.

I have made personal contribution in the second and the third area and therefore the discussion will be slightly biased towards my own work. The first area of instabilities, however, is fascinating in terms of the bizarre behaviour one can obtain and has been therefore specially highlighted.

Instabilities in viscoelastic flows through contractions

Very interesting instabilities can be found in a variety of situations involving flows of polymer fluids. These have been recently reviewed by Larson[16] in an excellent

manner. We will be concerned only with some specific aspects of instabilities here.

The instabilities found in viscoelastic fluids flowing through contractions are of potential importance in molding, extrusion, and in fibre spinning, since each of these processing operations involves contraction flow at some stage. For instance in fibre spinning, polymeric fluid is forced through a 'spinneret', which is a plate with an array of orifices.

The geometry of the cylindrical sudden contraction is depicted in Figure 7. The fluid enters the contraction region from an upstream tube of radius R_1 and is accelerated into a smaller tube of radius R_2. For any fluid, Newtonian or non-Newtonian, there exists a region of extensional flow near the centerline and the contraction plane, and there is a secondary flow consisting of an eddy in the salient corner.

For a Newtonian fluid inertia can change the flow and the shape of the salient corner vortex[17,18]. Many interesting transitions occur for viscoelastic fluids as the flow-rate is increased and flow is thereby made more elastic. The earliest visualization studies in the planar contraction are those of Giesekus[19], while early studies in axisymmetric contraction were made by Cable and Boger[20–22]. In these and later studies[23,24], a complicated series of transitions has been found, the details of which depend on the specific fluid and on the geometric parameters of the contraction, especially the contraction ratio R_1/R_2. Always, however, at $De = o(1.0)$, there is an enlargement of either the corner vortex, or of a second vortex that often appears near the lip of the contraction. Here, the *Deborah number De* is defined as $De = \bar{V}_2 \lambda / R_2$. At higher Deborah numbers, these workers have observed that the greatly enlarged vortex either pulsates regularly, or becomes asymmetric and spirals around the upstream tube. Finally, at $De = 15$, the oscillations become aperiodic[24].

In Laser–Doppler velocimeter studies of McKinley *et al.*[24] and of Lawler *et al.*[25], the first transition with increasing De produced a time-dependent flow. In fact it occurred before the onset of the visible pulsing of the enlarged vortex. These Laser–Doppler studies show that at least in some cases, three-dimensional time-periodic oscillations in velocity occur in a confined region near the lip at a critical Deborah (De_c) below the regime of vortex enlargement. As De is increased above De_c, higher harmonics and even a subharmonic can appear in the frequency spectrum. At still higher De, in the work of McKinley *et al.*, a lip vortex appeared. The velocity field associated with this lip vortex was quasiperiodic for small $R_1/R_2 (\leq 5)$ and was steady for larger R_1/R_2. At still higher De, in the vortex growth regime, the frequency spectrum showed the flow to be aperiodic for $R_1/R_2 \leq 5$. Figure 8 shows the flow transitions determined in the Laser–Doppler and visualization studies of McKinley *et al.* The sequence of transitions that occurs in axisymmetric contraction flow is sensitive to both the contraction ratio and the fluid rheology.

Shaping of polymer objects depends crucially on the instabilities during flow. When a polymeric fluid is

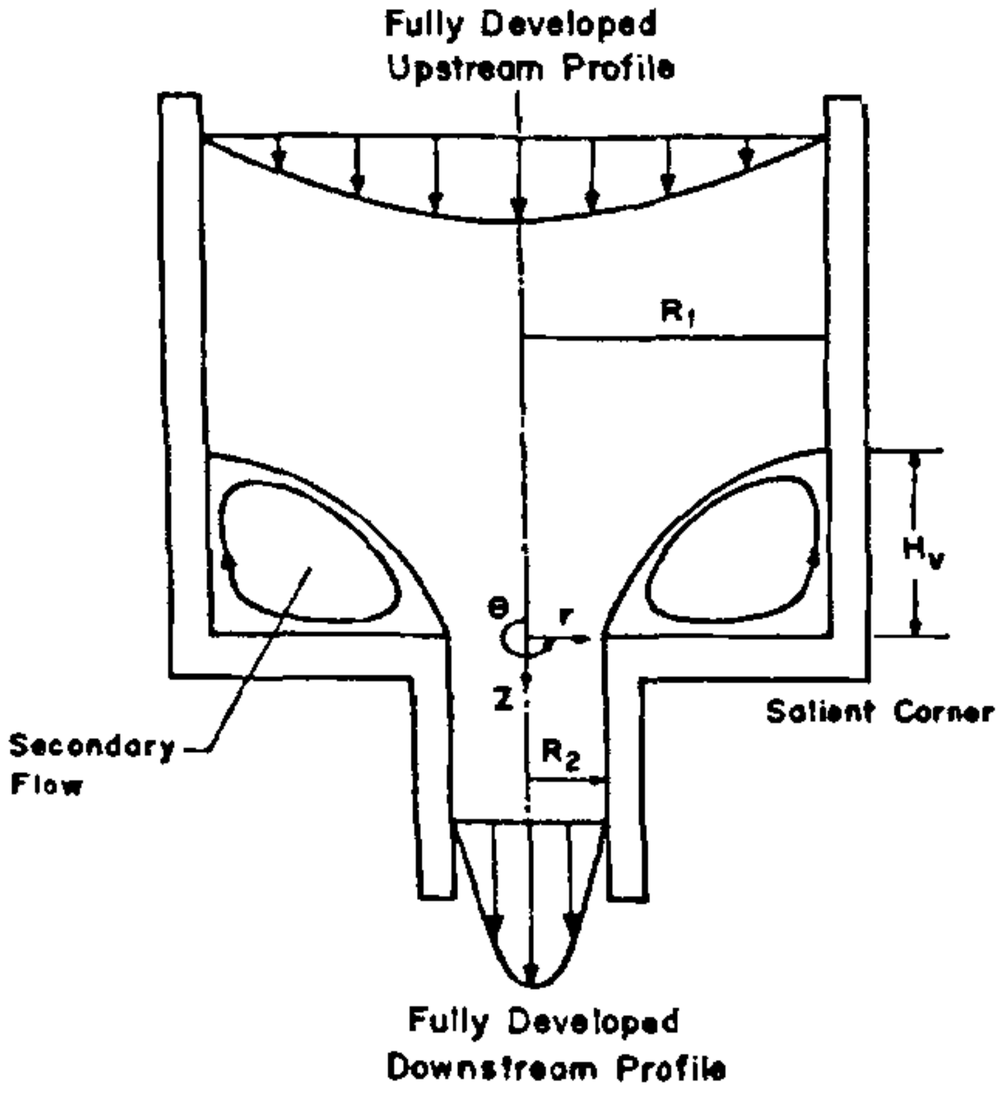

Figure 7. Geometry of axisymmetric sudden contraction flow.

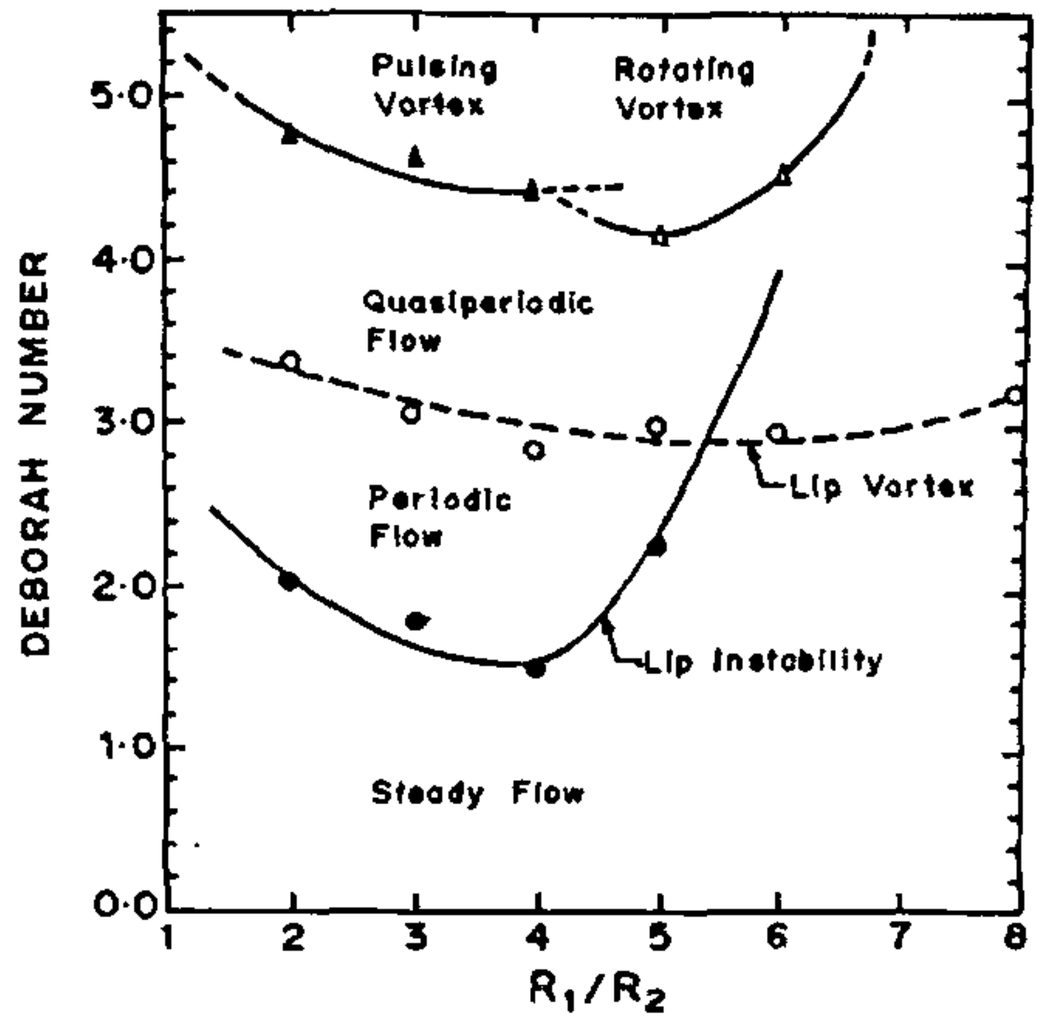

Figure 8. Flow transition diagram for sudden contraction flow of a solution of 3100 ppm polyisobutylene ($MW = 1.2 \times 10^6$) in low-molecular-weight polybutene with little added tetradecane (from McKinley *et al.*[24]).

forced through a capillary or slit die, distortions of the extrudate are observed when the recoverable shear S_R reaches a critical value in the range 1–10 (refs. 26, 27). The recoverable shear $S_R = \tau_w/G$ is defined as the wall shear stress τ_w divided by the characteristic elastic modulus G. The wall shear stress τ_w is proportional to the average pressure gradient in the die, $\Delta p/L$, where Δp is the pressure drop along the die and L is its length. The modulus can be obtained from $G \approx \eta_0/\lambda$, where η_0 is the zero-shear viscosity and λ is a characteristic relaxation time. Hence $S_R \approx \dot{\gamma}$ is approximately equal to the Weissenberg number. The distortions that occur can range from loss of gloss[28], small scratches, or slight roughness[29] to massive aperiodic and unsymmetric variations in cross-sectional area and shape[30]. While the origins of extrudate distortions are still in dispute, there is agreement that less severe distortions, often called *sharkskin*, ought to be distinguished from more severe distortions that are often called *gross fracture* or *wavy fracture*[27].

As the name implies, sharkskin is a *surface* roughness that usally modulates the extrudate diameter by no more than one per cent or so (see, however, ref.31). Figure 9 shows different instabilities observed by Piau *et al.* in a schematic way. Sharkskin consists of semiregular cracks of grooves that run mainly perpendicular to the flow axis. Gross fracture typically involves diameter variations of 10% or more, which at high flow rates are extremely irregular, even chaotic. In addition, some materials show, in cylindrical dies, a fracture regime with regular large-amplitude helical distortions. Piau *et al.*[29] have provided an excellent study of these features of unstable flow of viscoelastic liquids.

Sharkskin and gross fracture are distinguished not only by the appearance of the extrudate, but also by the critical conditions for onset and by the character of the accompanying flow inside the die. Gross fracture occurs when the wall shear stress reaches a critical condition that seems to depend only on the polymeric fluid and little or not at all on the die diameter, its length, or the material from which it is made[29,31,32]. Sharkskin, on the other hand, does not occur for all polymeric fluids[33], and for those for which it does occur, the onset condition has been found to depend on the shape of the outlet region of the die[29], the length of the die [34] and in some cases on the material of construction or coating on the exit region of the die[28,34]. Sharkskin occurs at a flow rate lower than that required for gross fracture [32]. At the onset of gross fracture for polymers without long-chain branching, there is nearly always a sharp change in slope of the curve of flow-rate versus pressure drop[27,31,32]. Often the curve becomes vertical or nearly vertical in the gross fracture regime, while at the onset of sharkskin, the change of slope is much smaller.

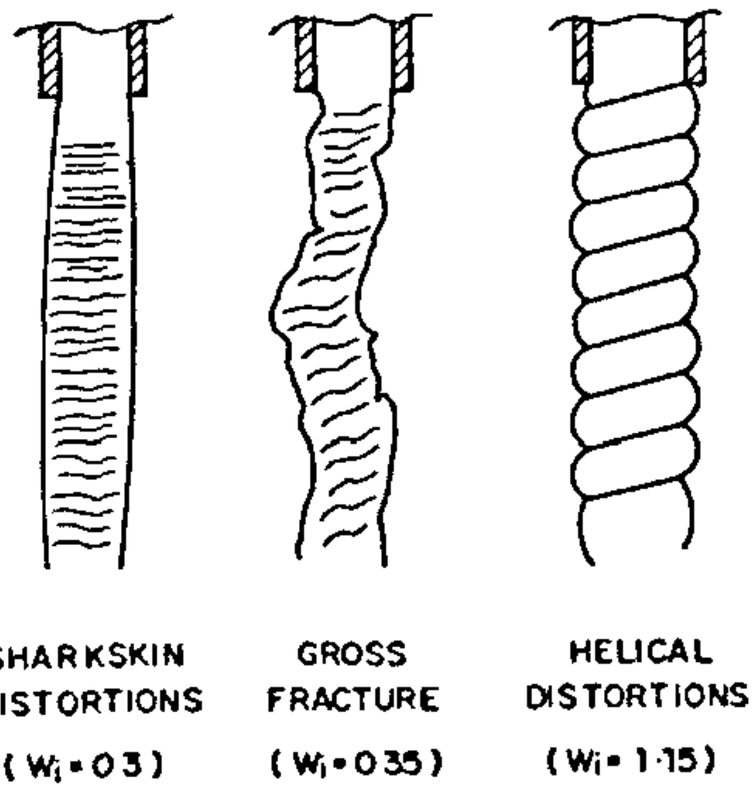

Figure 9. Flow through a cylindrical orifice. *a*, Sharkskin distortions of a branched polydimethylsiloxane ($MW = 4.3 \times 10^5$ at $Wi = -0.3$). *b*, Gross fracture of the same melt as (a) at $Wi = 0.35$, *c*, Helical distortion of a linear polydimethylsiloxane ($MW = 1.3 \times 10^5$) at $Wi = 1.15$. (Schematic diagrams based on the work of Piau *et al.*[29].)

In silicon polymers, Piau *et al.*[29] found a regime of helical fracture between the sharkskin and gross-fracture regimes, and they also found a regime of surface scratches parallel to the flow axis at pressure gradients lower than those required for sharkskin. In flows driven at constant upstream mean velocity, Ramamurthy[28], Kalika and Denn[32] found between sharkskin and gross fracture a region of 'stick-slip' or 'cork flow' characterized by alternating distorted and smooth extrudate, with a period of alternation roughly equal to the residence time of the melt in the die. The pressure drop in the die also oscillated with the same period, while the flow-rate that was nominally kept constant by the steady displacement of a plunger that forced the melt through the die oscillated at the die exit because of volume expansion and contraction of the melt caused by the severe pressure oscillations.

With our understanding of the rheological behaviour of these materials, can these phenomena be explained? Explanations for extrudate distortions usually invoke either failure of adhesion of the polymer to the die, or mechanical failure of the polymer itself. These explanations are referred to as wall slip and constitutive instabilities respectively[33]. Wall slip is often modelled by replacing the conventional no-slip boundary condition by one that allows a fluid velocity at the wall that depends on shear stress or strain history of the fluid at the wall[35–37]. A constitutive instability, on the other hand, will occur if the constitutive relationship between shear stress and rate of shear is non-monotonic[38] as depicted in Figure 10. Although these two mechanisms of extrudate distortion are different in principle, they are in practice difficult to distinguish, because both predict the same macroscopically observable phenomena of sudden increase in flow-rate at a critical pressure

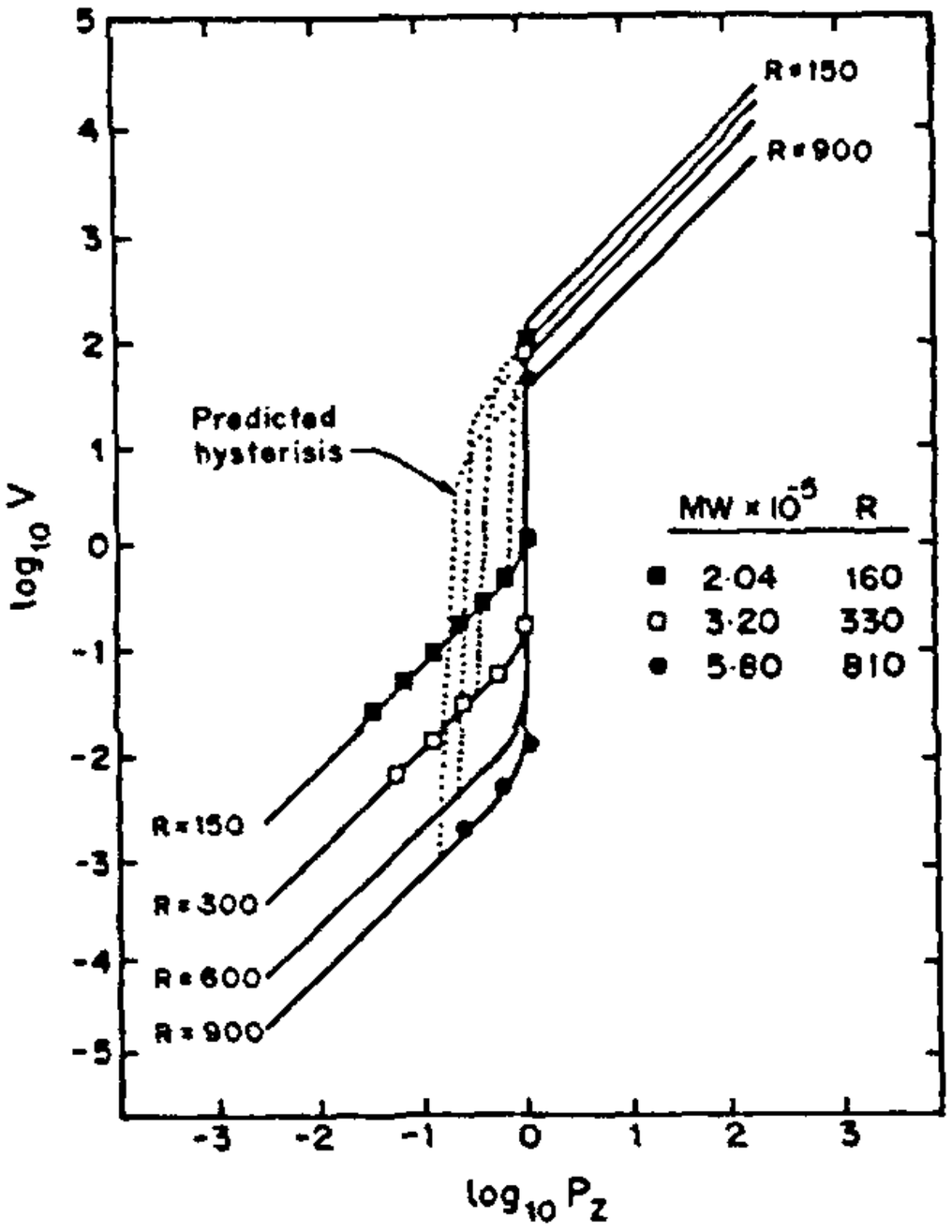

Figure 10. Theoretical curves of flow velocity (V) vs pressure (P) computed by McLeish and Ball[40] using an extended Doil-Edwards equation, (R = ratio of reptation to Rouse relaxation time). Experimental data are by Vinogradov[45].

drop. Furthermore, they both seem likely to lead to flow instabilities and extrudate distortion.

By using flow visualization or by measurements of rates of heat transfer at the die-fluid surface, it has been possible to infer that in the gross fracture regime the flow in the die is nearly plug flow, or intermittently plug flow[30,31,39]. This evidence lends support to the slip hypothesis, but theories involving constitutive instabilities usually predict that the material will develop a thin layer near the wall, at which shear rates are high, while most of the material moves in a plug-like fashion[40]. Also, since extrudate distortion is only seen in viscoelastic fluids, if adhesive failure is occurring, its occurrence evidently requires a high level of molecular orientation in the fluid. This point is reinforced by the observation that entangled polymer solutions, like melts, show gross fracture when the recoverable shear S_R (which is a measure of molecular orientation) reaches 2–5 (ref. 41). This holds for entangled solutions even when the polymer concentration is low enough that the modulus G and, consequently, also the critical wall shear stress are two orders of magnitude lower than the critical wall shear stress required for gross fracture of melts. Thus, in entangled solutions or melts, high levels of orientation are not only required, but also are sufficient for gross fracture to occur. Any wall slip mechanism for gross fracture must, therefore, involve the constitutive properties of the fluid.

To date, no theory has been developed that is able to predict such distinguishing features of extrudate distortions as the spectrum of wavelengths or frequencies of the distortion, or their amplitudes. However, the Doi–Edwards molecular theory for entangled polymers does imply that a constitutive instability, or catastrophic failure of the fluid's viscous resistance to flow through the die, will occur when S_R is roughly 2 or so[40–43]. A similar failure should occur in other shear flows such as cone-and-plate flow. Indeed, fracture-like phenomena have been reported in these geometries as well. A constitutive instability at $S_R = 2$ is expected from the Doi–Edwards theory because it predicts a non-monotonic stress-shear rate curve such as that shown in Figure 10 and not the stress minimum at higher shear rates. But the stress minimum can be included in the theory by accounting for a transition to 'Rouse-like' or unentangled flow behaviour when the shear rate reaches a value roughly equal to $1/\lambda_{Rouse}$, where λ_{Rouse} is the longest Rouse relaxation time. From an analysis of such an extended Doi-Edwards model, McLeish and Ball[40] have been able to predict features of the spurt phenomenon in the nearly monodisperse polybutadiene and polyisoprene melts[44,45]. In particular, they have predicted the critical condition for spurt and the dependence on molecular weight of the magnitude of the jump in flow-rate that occurs at the critical condition.

The idea that gross fracture is caused by a constitutive instability is therefore supported by the observation that it occurs in virtually all highly entangled polymeric liquids at a value of S_R close to that predicted for the onset of severe shear thinning by Doi–Edwards theory. Additional support for the idea can be found in the observation that critical value of S_R is increased substantially when the fluid is unentangled and thus much less shear thinning. Entanglements disappear either when the polymer molecular weight is low, or the solution is dilute. In both cases[24,44], spurt or grossly unstable flows are delayed or eliminated. However, molecular theory would also suggest that non-monotonic relationships between stress and shear rate could be avoided by using polydisperse melts, with distribution of relaxation times. But gross fracture has frequently been observed in highly polydisperse melts. This observation seems to be at odds with the idea of constitutive instabilities as a cause for melt fracture.

Some general comments on instabilities are in order. The influence of viscoelesticity on hydrodynamic stability is quite varied. In dilute unentangled or moderately entangled polymer solutions, the first normal stress difference N_1 is a driving force for

instability in shearing flows with curvilinear streamlines. At a critical value of the Weissenberg number, (proportional to the ratio of N_1 to the shear stress τ_{12}) such instabilities have been shown to occur in cone-and-plate, plate-and-plate, and Taylor–Couette flows. Instabilities in these latter two flows should produce viscoelastic analogues of Taylor–Dean and Gortler vortices, respectively. Viscoelastic instabilities in these polymer solutions also occur in flows with strong extensional and shearing components; namely contraction flow, flow around a sphere, and flow around a cylinder. In these, the secondary flow at onset is confined to a region near the stagnation point.

In concentrated, entangled solutions and melts, these instabilities seem to be rare or nonexistent. Theoretical work shows that curvilinear shearing instabilities are suppressed by shear thinning of Ψ_1 and especially by the negative second normal stress difference that characterizes the rheology of well-entangled systems. However entangled fluids display a different class of instabilities, namely fracture. The severe form, called gross or wavy fracture, typically occurs in or near the shear-thinning regime at a value of the Weissenberg number in the range 1–10. In Poiseuille, cone-and-plate, or plate-and-plate flows, severe fracture manifests itself as distortions in fluid-air surfaces, in sharp or discontinuous changes in the stress-flow rate curve, and in macroscopic slip or plug-like flow. Although fracture was first observed decades ago, the mechanism by which it occurs is not fully understood. The failure of adhesion between the polymeric fluid and the wall has been extensively cited as a cause. The overall evidence indicates that the rheology of the bulk fluid plays a major role in gross fracture, while slip at the wall plays a role in less severe forms of fracture, such as sharkskin.

Elastically-driven instability is still far from understood properly. This is not only due to the limitation of the constitutive equations, but also because secondary flows resulting from the instabilities are typically time-periodic and/or three-dimensional, and often contain a wide spectrum of wavelengths and frequencies. Ideal cases, in which the first instability experienced by the base flow is stationary and either two-dimensional or axisymmetric, exist in Newtonian Taylor–Couette or Rayleigh-Benard flows, but are rare or nonexistent in elastically driven instabilities.

Thus one can emphasize that for Newtonian fluids one can compute not only complex multidimensional steady flow fields, but also the disturbances to which these flow fields are linearly unstable. One day one should be able to do similar analysis for multidimensional viscoelastic flows. We have not been successful in this endeavour, because computing even the stationary base flows at Weissenberg numbers of order unity or higher has until very recently been difficult, and the accuracy of the few solutions obtained has been questionable[46]. But with recent advances[47] it seems likely that numerical stability analyses of multidimensional viscoelastic flows will soon be common. Hopefully, this will enhance our understanding in an important area, which is so vital for controlling the polymer-processing operations.

Particle motion

The process of mass transfer in dispersion of bubbles or drops is wholly governed by the mechanics of bubble or drop *formation*, rise, deformation, coalescence, break-up, etc. Each of these processes needs to be understood fundamentally. Some of our early work was focused on looking at the aspects of particle motion in non-Newtonian fluids.

The drag on a solid sphere moving under creeping flow conditions in non-Newtonian fluids is given by

$$C_D = \frac{24x}{\mathrm{Re}} \tag{21}$$

Here x is a correction factor, which accounts for the non-Newtonian character of the fluid. $x=1$ for a Newtonian fluid. In the late sixties and early seventies, there was a flurry of activity to calculate this correction factor by solving the relevant equations of motion. There was a dispute as to whether $x<1$ or $x>1$ for shear thinning fluids, whose power law index (n) was less than unity. In 1976 we published a paper[48], which provided a simple but approximate analytical solution to the problem of a sphere moving in mildly pseudoplastic fluid. Interestingly enough, the problem of calculation of drag on a sphere moving in a non-Newtonian fluid continues to draw attention even today[49].

The motion of spheres under laminar conditions but at larger Reynolds numbers poses interesting problems. The well-known separation phenomenon, which leads to the formation of a wake behind the sphere, has been well analysed in the literature for Newtonian fluids but has been very poorly understood for non-Newtonian fluids. We showed[50] that the wake behind a sphere is completely eliminated in elastic liquids. We not only demonstrated delayed separation in elastic liquids but also showed evidence for the formation of an unusual double wake (see Figure 11). In fact this is the only paper in the literature to date which quantitatively analyses the influence of elasticity on the formation of wakes for solid spheres moving in elastic liquids.

We used inspectional analysis in this paper to predict the separation point. We correctly predicted that for shear thinning materials, there will be a delayed separation. However, we were wrong in our prediction of the influence of elasticity. Our analysis failed to

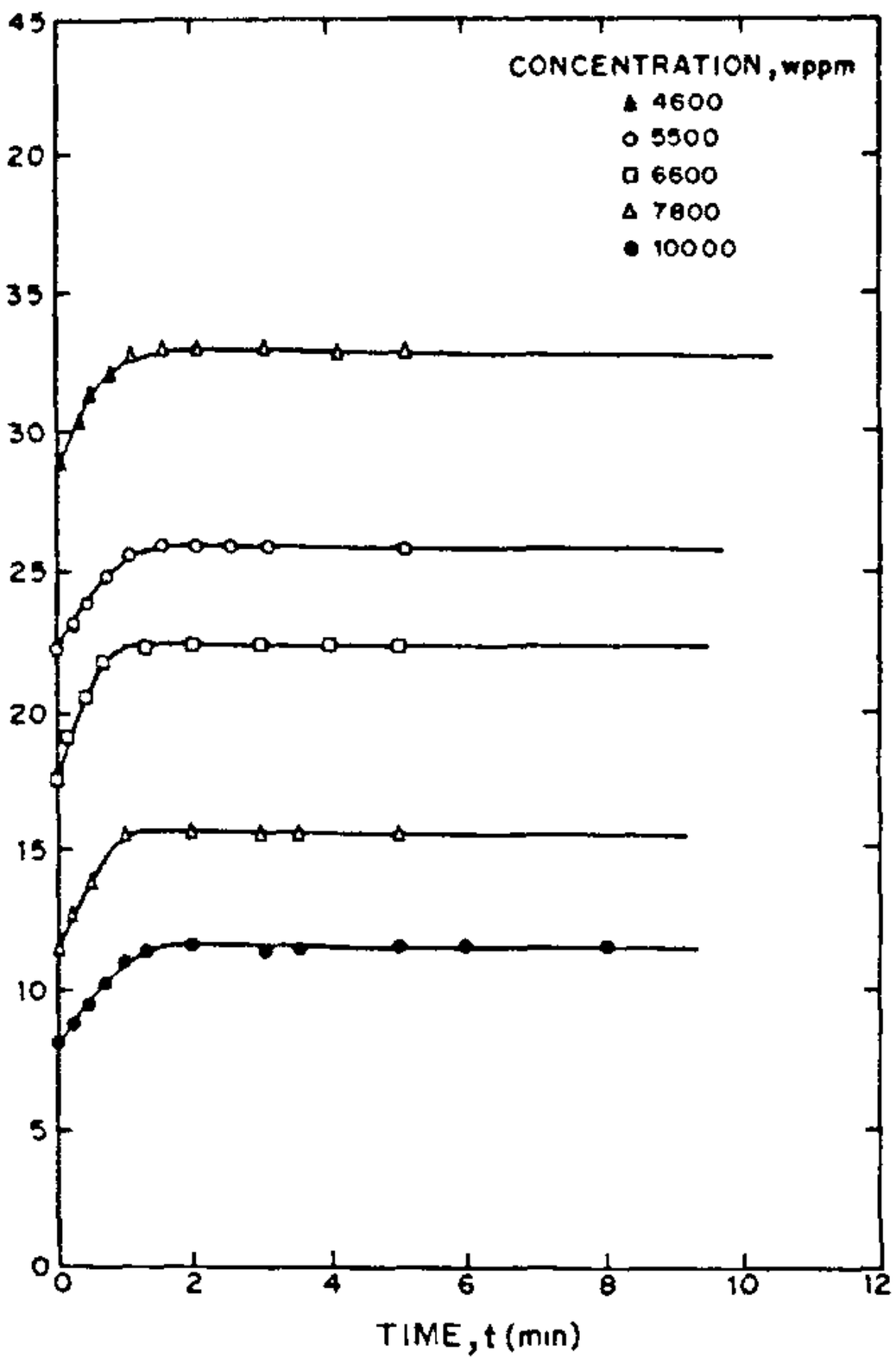

Figure 11. Time-dependant terminal velocities for the fall of a single sphere in polyacrylamide solutions reported by Ambeskar and Mashelkar[52].

predict that viscoelasticity would move the point of separation to the rear stagnation point. The problem remains unsolved even today!

As though this complexity is not enough, there appear to be further complications in the movement of solid spheres in elastic liquids. Ambeskar[51] showed that even under steady state conditions the terminal velocity of solid spheres moving through viscoelastic fluids can show an intriguing behaviour. The phenomena can be simply explained. Supposing we drop a sphere in a viscoelastic fluid and measure its terminal velocity. We then wait for few hours and drop another sphere. We will find that the velocity of the sphere is exactly the same. On the other hand if the second sphere is dropped a few seconds after the first sphere has passed through, then one actually finds that the terminal velocity of the second sphere is larger. If we continue such sphere-dropping experiments for long enough time then there will be a point beyond which the velocity will not change. Figure 11 shows typical data presented by us recently[52].

One of the explanations that was advanced for this phenomenon was that macromolecules under stress move away from highly sheared regions. (We will be making a detailed reference to this later on.) It is easy to see that if this did indeed happen then the depletion of concentration of macromolecules in the line of the moving sphere will create a low viscosity layer and therefore the drag force will reduce. We subjected this hypothesis to test. Careful withdrawal of a solution from the centre and measurement of centreline concentration showed that there was no such depletion at all. What is particularly disturbing is that the relaxation time for such fluids is small compared to the actual restoration time, which is the time that the fluid takes before the sphere velocity gets restored to the original velocity. For instance, the range of fluid relaxation times is of the order 10^{-1} s to 20 s, whereas the characteristic restoration time is of the order of 9 to 10 min.

A related problem comes up when some elementary problems in suspension rheology are considered. The problem of interactions between two spheres falling along their lines of centre in a viscoelastic fluid was studied by Birds' school[53]. They found that for 'small' initial separations of the spheres, the two spheres eventually converged. However, for 'large' initial separations the two spheres eventually diverged! This led Bird and coworkers to the definition of a critical initial separation distance. From this quantity the characteristic time was derived for the two spheres system. Bird's school presented this as an interesting finding but provided no possible explanation of the phenomenon. The possible findings on time-dependent terminal velocity presented by us and Bird's group's findings are related. The exact quantitative analysis is somewhat unclear though.

Consider now the motion of bubbles and drops. Small bubbles behave as solid spheres. We analysed the bubble motion under creeping flow conditions in power law fluids and also Bingham fluids, which show a yield stress[54,55]. The predictions looked reasonable when compared with the experimental data.

Slightly larger bubbles show an inverted tear drop shape. Although studies on deformation of fluid particles in Newtonian liquids are available, the distortion of a spherical bubble to a tear drop shape has still not been shown by exact computations. Our later work[56] on deformation and shape of bubbles was semi-empirical.

What is particularly fascinating is the phenomenon of discontinuity in velocity. This spectacular result, which was first observed by Astarita and Apuzzo[57] and subsequently confirmed by many workers, which included our group too[56], still remains unexplained. Figure 12 shows the dramatic evidence of a discontinuity in the velocity of rise-bubble volume relationship

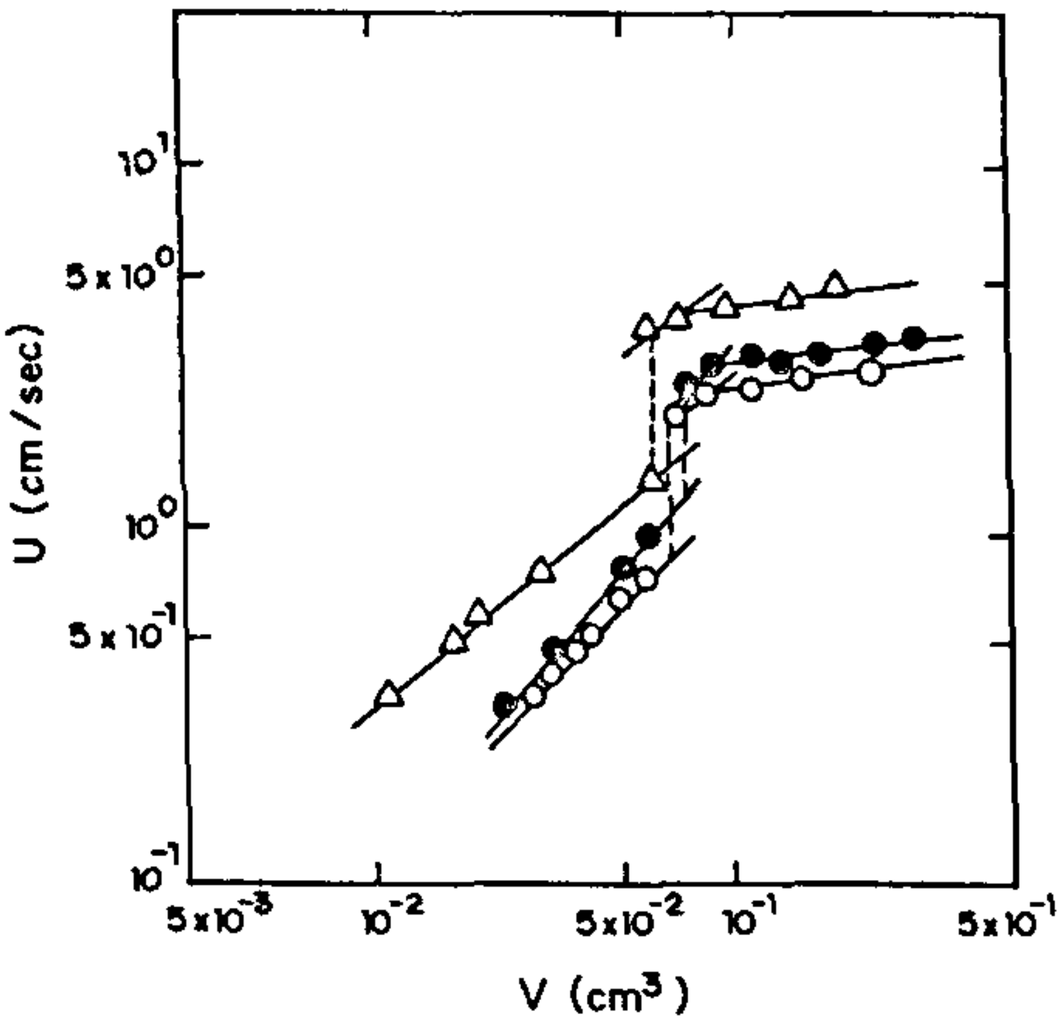

Figure 12. The discontinuities in the velocity–volume plot for gas bubbles in viscoelastic liquids observed by Acharya *et al.*[56] (○ = 0.5% polyacrylamide in glycerol, ● = 0.5% polyacrylamide, Δ = 0.5% polyethylene oxide.)

for elastic liquids. Astarita and Apuzzo[57] suggested that the predicted transition could be explained on the basis of a change of Stokes regime (rigid interface) to a Hadamard–Rybczyski regime (free interface). We showed[56] with a simple criterion for a change of rigid to free interface proposed by Bond and Newton[58] that the transition occurs at a critical bubble radius = $(\sigma/\rho g)^{1/2}$. Here σ is the surface tension, ρ the density and g the acceleration due to gravity. However, no rational explanation for this phenomenon exists even today. The concern that we have is whether the time-dependent effects that we have reported again have a significance to the problem of discontinuities that we are observing. The large restoration times reported by Ambeskar and Mashelkar[52] would imply that unless experiments are done in fluids on time-scales much larger than the restoration times, we may get spurious results.

For large drops or bubbles (mercifully!) the inertia terms dominate both the viscous and elastic terms in the equation of motion. The velocity fields are therefore essentially the same as in Newtonian and non-Newtonian fluids. We have shown[59] that the wave theory developed originally for inviscous fluids can be successfully used for predicting the drag for the motion of Newtonian liquid drops in non-Newtonian liquids and also for the motion of non-Newtonian liquid drops in Newtonian liquids. Our photographic studies[59] showed that wakes behind liquid drops were much larger in elastic liquids. We thus have an interesting set of findings. For a rigid interface (solid sphere) the wake gets eliminated. For a mobile interface (liquid drop) the pattern is exactly in the opposite direction. We still do not have a rational model to explain this.

When a gas bubble moves upwards in a liquid there is a wake behind the bubbles. When some liquid is pushed ahead in front of the bubble more liquid is pulled along behind the bubble. Hassagar[60] got an unexpected result when he studied the wakes behind bubbles in elastic liquids. He showed that the velocity behind the bubbles is in the downward direction, i.e. away from the rising bubble. This is amounting to the formation of a 'negative wake'. This interesting observation has a consequence in coalescence. It implies reduction in rates of coalescence when two bubbles move together. We do not still know as to why the movement of a bubble produces a negative wake.

We have shared the simplest problem of motion of a single gas bubble or a liquid drop or a rigid sphere and shown that we have still not resolved these simple problems in spite of all the advances we have made in non-Newtonian fluid mechanics! We will elaborate this point further by considering another apparently simple flow, namely that of a dilute polymer solution past a tiny cylinder.

Rapid external flows of viscoelastic materials past submerged cylinders

We specifically take up the simple problem of external flow of a very dilute polymer solution in which a very high-molecular-weight polymer (such as polyethylene oxide) is dissolved at a concentration of few parts per million level. We look at the flow as the fluid flows past tiny cylinders. The objective is to find out the drag coefficient and the heat and mass transfer coefficient in such situations at low to moderate Reynolds numbers. At first sight, this looks to be a very simple problem. After all, one feels, addition of a few parts per million will bring no magic changes. But there are surprises waiting even in this case.

The interesting anomalies in this problem were first detected by James and Acosta[61], when they tried to study turbulence in viscoelastic fluids. Their aim was to use hot wire anemometry for turbulence measurements in dilute viscoelastic liquids. By measurement of the rate of loss of heat from a wire, it is easy to compute the local velocity distribution, since as the velocity increases, the rate of heat loss increases directly. This relationship enables one to obtain the local velocities through a suitable calibration. However, they found some truly surprising results, as can be seen from Figure 13. In the case of a Newtonian fluid, the rate of heat transfer changes continuously with velocity. However, in the case of a dilute polymer solution, after a critical velocity is reached, the rate of heat transfer

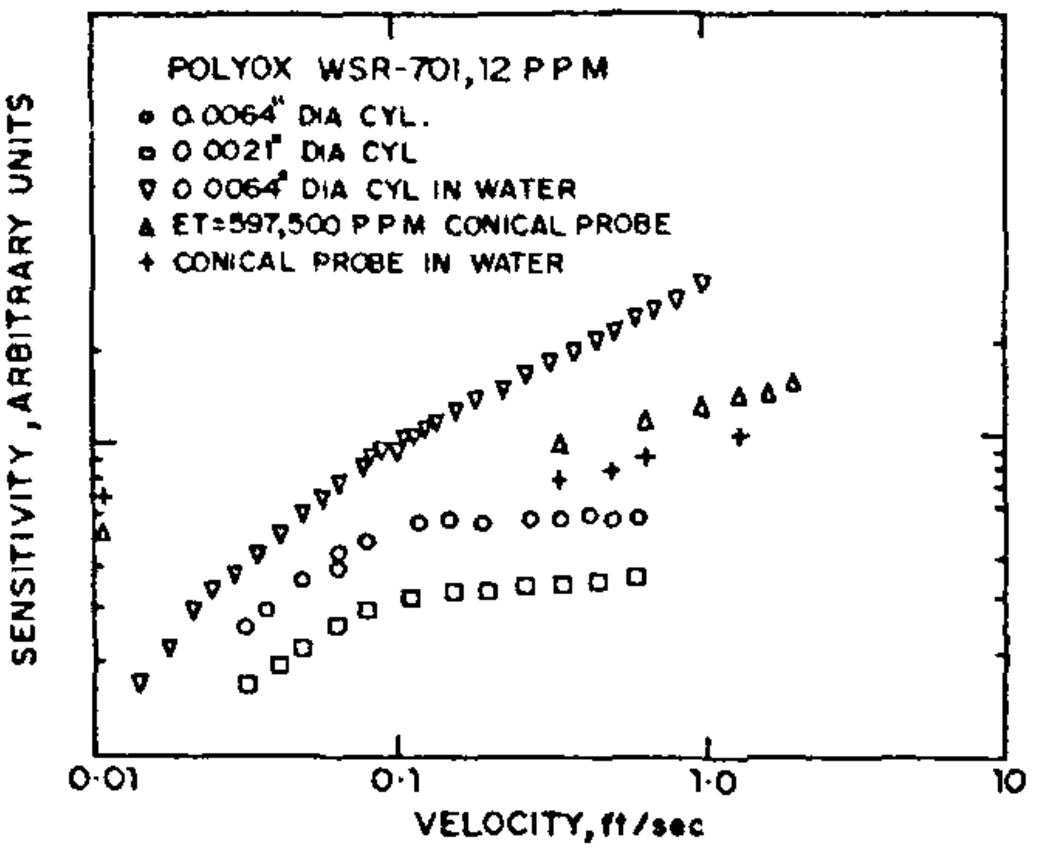

Figure 13. Comparison of heat transfer rates of Newtonian and viscoelastic fluids. The data have been reproduced from the paper by Metzner and Astarita[63].

becomes independent of the velocity! Interestingly enough, if the probe is not a blunt object such as a cylindrical wire, such phenomena do not take place. The parallel data on drag coefficients (see Figure 14) obtained by James and Gupta[62] also show the same behaviour. These findings in the late sixties excited quite a few of us and we all made attempts to interpret these phenomena. The last effort I know was a paper presented by Dan Joseph of Minnesota University at the 62nd Annual Meeting of the American Society of Rheology during October 1990 in New Mexico! It is interesting to go through the history of this development and summarize the variety of models that have been proposed to explain this phenomenon.

The first authors to make an attempt to explain this

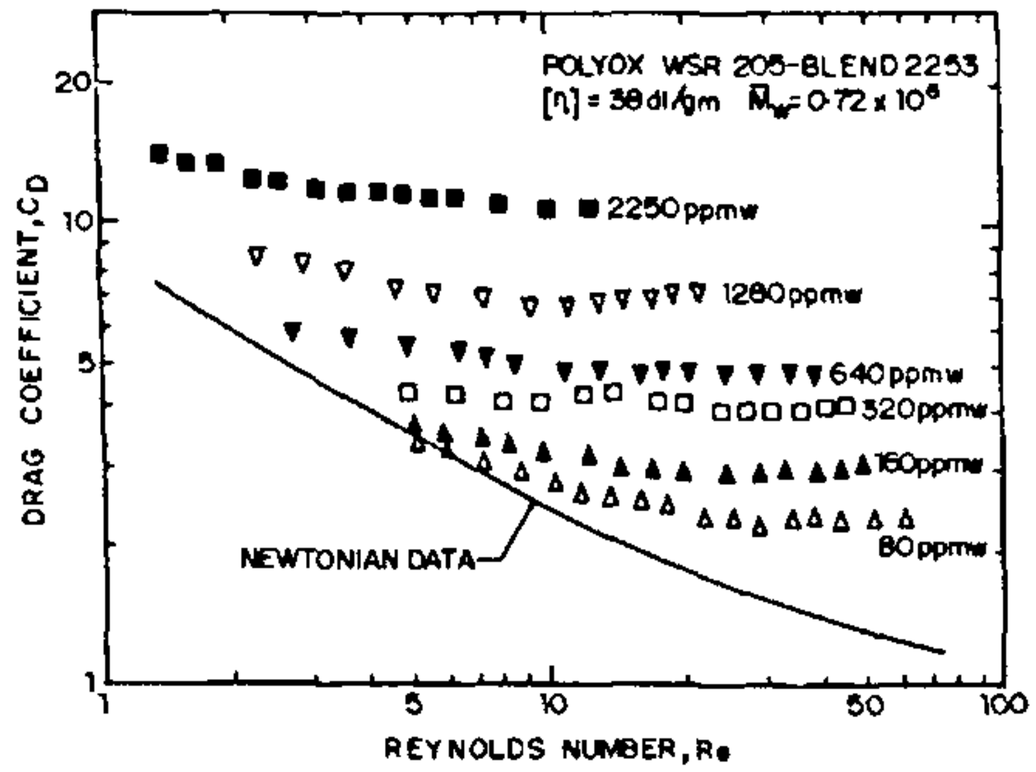

Figure 14. Comparison of drag coefficients in Newtonian and viscoelastic fluids Cylinder diameter = 0.006 inch. The data reported by James and Gupta[62].

phenomenon were Metzner and Astarita[62]. They analysed the boundary layer flow of an elastic liquid past a cylinder. They argued that near the front stagnation point of the cylinder, the rates of deformation change very dramatically. Such deformational processes may be characterized by large values of Deborah number. They argued that at high external fluid velocities, a Deborah number of sufficient magnitude to imply solid-like material response will be expected. If this happened, then there will be a tendency towards the development of a block of solid-like stagnant material coating the region surrounding the stagnant point. This would imply a region surrounding the physical stagnation point, in which fluid velocities, though not zero, will be in fact substantially below the free stream velocity.

To model the flow near the front stagnation point, which had extensional flow characteristics, they assumed that the stresses developed in the stretching of a flat sheet could be considered to a first approximation. These are given by the expression:

$$\Delta \tau = \frac{4\eta\Gamma_s}{1-(2\lambda\Gamma_s)^2} . \tag{22}$$

Here $\Delta \tau$ is the stress difference, η the viscosity of the fluid, Γ_s the rate of stretching and λ the relaxation time. They argued that the maximum possible stretching rate will be limited by the requirement that the stresses remain finite. This means

$$\Gamma_{max} = \frac{1}{2\lambda} . \tag{23}$$

The stretching rate for a fluid flowing past a cylinder would be approximately given by

$$\Gamma_s = \frac{4U}{d}\cos\theta . \tag{24}$$

This implies

$$\left(\frac{U}{d}\right)_{max} = \frac{1}{8\lambda\cos\theta} . \tag{25}$$

Here U is the free stream velocity, d the diameter of the cylinder, λ the relaxation time and θ the angle measured from the front stagnation point. The significance of this equation is that it fixes the maximum value of the free stream velocity, at which, for a given cylinder diameter, potential flow may be maintained. If this maximum velocity is exceeded, then the external flow will depart from that of a potential velocity field in such a direction as to maintain the fluid stretch rate below the maximum level given by equation (25). This effect is essentially manifested as a thickening of the boundary layer through an increase in the effective radius of curvature of the external velocity

field in which a potential flow distribution may be assumed.

The major problem in this argument of 'limiting stretch rate' was that the level of stresses implied by Metzner and Astarita could be reached only under certain conditions. For instance, Denn and Marrucci[64] performed an analysis of the stretching of a flat viscoelastic sheet under unsteady conditions and showed that large stresses will be reached only when the following conditions were satisfied

$$\lambda_t \gg 1 \text{ and } \lambda\Gamma \gg 1, \tag{26}$$

where t is the time that a material element is subjected to a stretch rate of Γ. A careful reanalysis of the situation will show that such conditions are not easily satisfied under the conditions of flow and therefore perhaps the arguments based on 'limiting stretch rate' were not tenable.

Ultmann and Denn[65] looked at the problem in a different way. They carried out an Oseen type of approximation for the flow of a fluid around a cylinder. They showed that the velocity distribution was then obtained in terms of a stream function Ψ, which obeys the following differential equation.

$$\left(\frac{1-U^2}{\nu/\lambda}\right)\frac{\partial^2\Psi}{\partial x^2}+\frac{\partial^2\Psi}{\partial y^2}+\frac{\partial^2\Psi}{\partial z^2}-\mathrm{Re}\,\frac{\partial\Psi}{\partial x}=0. \tag{27}$$

Here ν is the kinematic viscosity, Re the Reynolds number, x, y, and z dimensionless space co-ordinates, and U the unperturbed velocity. One may notice that if $U<(\nu/\lambda)^{1/2}$ the equation is hyperbolic and admits solutions with discontinuities along the wave fronts. Discontinuities of macroscopically observable quantities in viscoelastic liquids have been reported experimentally by Joseph and coworkers[66,67]. One also notices that the quantity $(\nu/\lambda)^{1/2}$ is a constant for any given fluid. Therefore anomalies are to be expected, when the flow velocity reaches a critical value, which is independent of the length scale of the flow field.

These arguments are indeed appealing. However, it is rather worrisome that inclusion into the constitutive equation of even a very small retardation time λ_R leading to

$$\tau+\lambda\frac{\delta\tau}{\partial t}=\mu D+\lambda_R\frac{\delta D}{\partial t} \tag{28}$$

smooths out the discontinuities as shown by Tanner[68]. It is thus seen that the predictions made by Ultmann and Denn very much depend upon the model that is used and therefore such an analysis has obvious limitations, which good models should not have.

We ourselves entered this area later. We did an alternative boundary layer analysis[69] for elastic fluids. In classical boundary layer analysis one equates the inertial stresses and the viscous stresses within the boundary layer. However, we argued that for rapid external flows of viscoelastic fluids we must equate the elastic stresses and the inertial stresses. We provided physical arguments to show as to why this should be so.

As we know, in the case of a Newtonian fluid flowing past an object of characteristic length L, the boundary layer thickness δ depends upon the inverse square root of the velocity as shown below:

$$\delta\sim(L\nu/U)^{1/2}. \tag{29}$$

However, our new ordering method yielded an unusual result for the boundary layer thickness given by

$$\delta_{el}\sim(\nu\lambda)^{1/2}. \tag{30}$$

We called δ_{el} as an elastic boundary layer. Clearly this boundary layer thickness is independent of the free stream velocity and depends only on fluid properties.

We analysed the heat as well as the momentum transport problem in this framework. There was a fair agreement with our predictions and the data. There were no adjustable parameters at all in these calculations. The relaxation time λ was also calculated on a molecular basis.

We were quite happy at this development since photographic measurements[70] had demonstrated the existence of stagnation regions predicted by us. However, a point of concern was that the phenomenon was observed by many workers not only at intermediate Reynolds numbers but also at low Reynolds numbers, for which our boundary layer analysis was clearly not valid.

This problem continues to draw the attention of the researchers. Some additional interesting observations were made by Ambari *et al.*[71]. They performed an analysis of mass transfer from a small cylindrical wire in a dilute polymer solution by using an electrochemical technique. They found the same results that were obtained with heat transfer and drag coefficient by others. They ascribed this phenomenon to the rapid stretching of polymer coils, which occurs when the extensional gradient in the upstream vicinity of the wire becomes equal to the reciprocal of polymer relaxation time. In fact they directly linked it to the coil-stretch transition that is supposed to occur when macromolecules are rapidly deformed.

What is perhaps more interesting is that they found that fluctuations arise at the point of transition. This results, they argued, in a hydrodynamic instability induced at the point of viscosity stratification around the cylinder. They showed that instabilities actually occur near the stagnation point of the stream.

What is important about the analysis by Ambari *et al.*, is that they not only offered a rheological explanation, which involves viscoelasticity of the solution explicitly, but also provided in parallel a molecular interpretation.

Recently, Hu and Joseph numerically simulated the flow of an upper convected Maxwell fluid past a circular cylinder. They showed that for a fixed Reynolds number, as the fluid elasticity increases, there is an increasingly larger downstream shift of the streamlines. At the same time there is a relatively small upstream shift. The distortion of the streamlines creates a wide region near the cylinder, where the velocity is low. This stagnant region grows with increasing elasticity. Interestingly, for a highly elastic fluid, the isovorticity lines jam together at the front shoulder of the cylinder, creating a vorticity shock. There exists a second high vorticity region away from the cylinder surface suggesting generation of vorticity away from the cylinder surface or behind the vorticity stock. A special feature of this analysis is the existence of a critical velocity $[=(\nu/\lambda)^2]$, at which the variation of the drag and heat transfer changes from a characteristic Newtonian variation to a flat response. This finding is consistent with Denn's calculation with a convected Maxwell model. It is obvious that the features of Denn's and Joseph's findings should be similar, since they use the same constitutive equation.

We can clearly see that after the initial findings of velocity independent momentum and heat transport coefficients about 25 years ago, we are still attempting to resolve these issues.

Stress-induced demixing

Another area, in which we have been seriously interested during the last few years, concerns the phenomenon of demixing in polymer solutions under stress. First of all we have a situation where a solution with uniform concentration, which is flowing through a channel, may develop a concentration distribution in the flow passage. Additionally, it might also happen that a homogeneous polymer solution, when subjected to stress, may actually show phase separation. This peculiar influence of stress is not to be seen in low molecular weight systems. The implications of such demixing phenomena in polymeric media are rather profound.

Our interest in this area essentially originated when we read some appealing arguments made by Metzner *et al.*[72]. Qualitatively his argument was that in a moving deforming fluid the dissolved macromolecules will become aligned and stretched. This will change their entropy and free energy levels. In any flow process, in which the stress or the rate of strain level varies with position within the fluid, the molecular orientation and extension and consequently the free energy will also vary with position. In order for the free energy at steady state to become independent of the position, compensating concentration gradients will be set up. The net result of all these processes will be able to cause the macromolecules to diffuse towards regions of low-stress levels.

In fact Metzner *et al.*[72] analysed the concentration difference in an adjoining stagnant stream (region 2) with concentration C_2 and a flowing stream (region 1) with concentration C_1 and showed that the concentration difference will be given by

$$\ln \frac{C_2}{C_1} = \frac{tr\ \tau}{2C_1 kT} . \tag{31}$$

Here k is the Boltzmann constant, τ the extra stress tensor and T the absolute temperature.

Since $tr\ \tau$ is always positive, this equation suggests that with increased intensity of the stress field, the concentration in the stagnant region will become increasingly higher.

Metzner *et al.*[73] circulated polymer solutions in well developed laminar flow through a 0.95 cm circular tube, with a concentric cavity in the tube wall separated from the main flow by a fine screen. They obtained three different data points for different values of C_1 and wall shear rate ($\dot{\gamma}$), as $C_2/C_1 = 1.05$ to 1.3, while the theoretical estimates were in the range 1.7–3.2. Tirrell and Malone[74] at the same time had applied similar considerations and shown theoretically the possibility of development of concentration gradients within the flowing stream.

In the early 'eighties', when this problem attracted our attention, we were struck by the kind of implications such behaviour would have in actual practice. Consider, for instance, a capillary in which a polymer solution was flowing with uniform radial concentration. It would become nonuniform by the time it left the capillary. This can be explained as follows. In a capillary, the shear rate varies from the wall to the centre. The shear rate is the highest at the wall and zero at the centre. Since the level of free energy depends upon the shear rate, it stands to reason that there will be a free energy gradient within the capillary. Thermodynamic dictates, however, that such free energy gradients cannot exist and the free energy must be the same everywhere. Therefore the macromolecules must move from a highly sheared zone to a zone of low shear at the centre and create a depletion layer. This implies that an otherwise concentrated polymer solution will slide over a low viscosity depleted macromolecular

solution at the wall. This is amounting to an 'apparent slip'. One suspected that such phenomena might be occurring in a number of different instances without one having realized it. If such concentration inhomogeneities were developing all the time, then were we justified in using the hypothesis of no slip at the solid surface? In fact we felt that this would be the feature for practically all 'structured' fluid, including suspensions. This worried us, since no slip hypothesis was routinely used for solving problems in structured fluids. The conventional calculations using traditional methods had apparently failed to provide the correct solutions. Such discrepancies were prevalent in the literature. Figure 15 shows the discrepancy between theory and experiment in capillary flow summarized in the paper by Dutta and Mashelkar[75].

Figure 16 shows the discrepancy between theory and experiment in coating flows obtained by Gutfinger and Tallmadge[76]. Apparently the conventional approaches were failing. We felt that there was something wrong with the conventional way of doing these calculations by assuming no slip at the surface. The influence of slip on convective diffusion in structured fluids was analysed by us in an oft-quoted paper[77], where we essentially provided a heuristic analysis.

The heuristic analysis was replaced later by a more detailed quantitative analysis. Consider the flow of a polymer solution in a capillary. The macromolecules that migrate away from highly shear regions will also tend to come back to the high shear region because of molecular diffusion. In fact if one examines such gradients in a tube then the radial diffusion flux J_r can be shown to comprise two contributions

$$J_r = D_0\left[C\frac{\partial F}{\partial r} + \Phi\frac{\partial c}{\partial r}\right]. \tag{32}$$

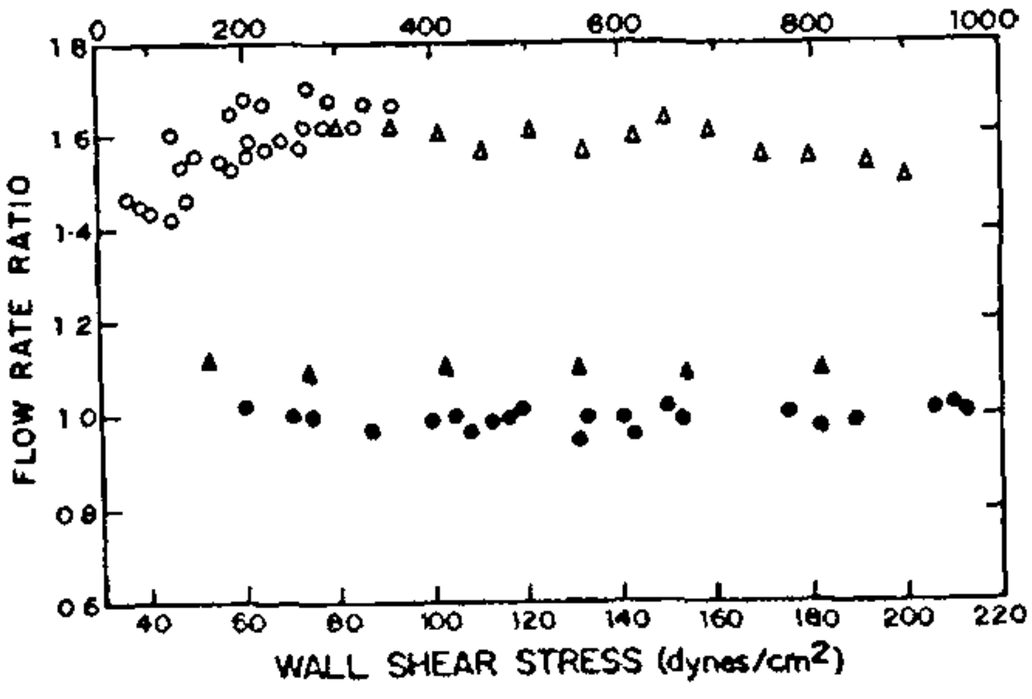

Figure 15. Flow rate enhancement (over that predicted theoretically) as a function of wall shear stress for low-molecular-weight fluids (closed symbols) and macromolecular fluids (open symbols). The data are for capillary as well as film flows. Upper scale is for shear stresses in falling film flow. The details can be seen in Dutta and Mashelkar[75].

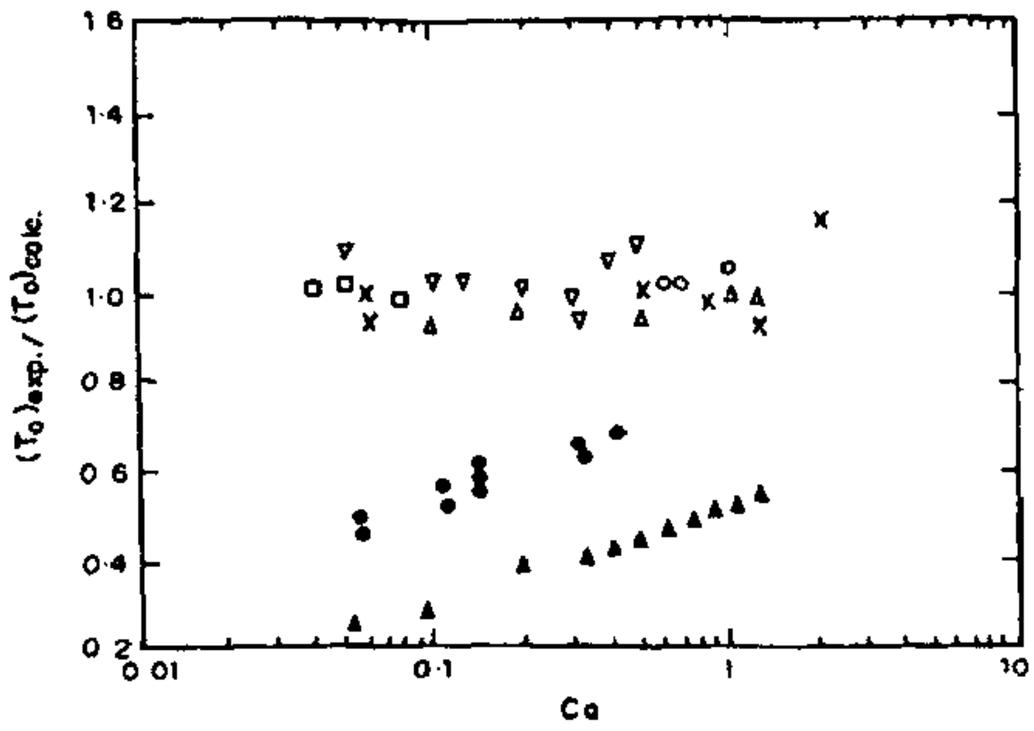

Figure 16. Comparison of experimental [(T_0) exp.] and calculated [(T_0) calc.] coating thicknesses for plate withdrawal. Open symbols are for Newtonian fluids and closed symbols are for non-Newtonian fluids. T_0 is the film thickness and Ca is the capillary number. Details in Dutta and Mashelkar[82].

The first is the entropic contribution resulting from a gradient of the chemical potential function caused by the deformation-induced free energy changes and the second is the usual Fickian contribution arising out of a concentration gradient. Here D_0 is the molecular diffusivity, c the concentration, F the chemical potential function, Φ a correction factor for concentration-dependent diffusivity and r the radial distance from the centre of the capillary.

The question then is that of getting the chemical potential function F. If the polymer molecules are assumed to be linear dumb-bells then this expression can be derived as

$$F = (\lambda\dot{\gamma})^2 - \frac{1}{2}\ln\left[1 + 2(\lambda\dot{\gamma})^2\right]. \tag{33}$$

This expression is valid, of course, for dilute solutions. The relaxation time λ can be obtained by rheological measurements. The important point to note is that F now depends upon the shear rate $\dot{\gamma}$. Therefore if there is a variation of $\dot{\gamma}$ across the radius then the term $\delta F/\delta r$ would be finite and we will have a positive contribution due to the forces of entropic origin.

We did more detailed mathematical analysis. The limiting case of full development in capillary flow was considered by us[75]. A detailed study of this problem was justified by the fact that it could provide information regarding the maximum extent of migration possible for a given combination of rheological properties and flow conditions. We solved the problem for the limiting case of a fully developed concentration field, which we called as FDCF asymptote. We argued that the size dependence of flow curve was the characteristic of the developing flow only. We showed, quite contrary to the prevalent belief then, that size

dependence is not necessarily a positive indication of slip. The observed similarity of concentration and velocity profiles for different capillary sizes implies that, under fully developed conditions, the flow curves (that means the shear stress–shear rate plots) depend only on the initial polymer concentration and not on the capillary size. This was contrary to the experimental observations. We also analysed[78] the role of stress-induced migration to explain the anomalies that were observed in falling films of dilute polymer solutions[79,80].

We later did a very rigorous numerical analysis[81] and took into account the strong interdependence between the flow field and the resulting concentration profile. We solved the problem of flow length required for stress-induced polymer migration in fine capillaries. We showed that to achieve a given extent of migration, which means a given extent of flow enhancement ratio, the flow lengths required were considerably less than predicted by prior analysis. In fact we kept on doing comparisons between the predictions of flow enhancement that we made and the experimental observations (see Figure 17). One can see that we have been able to rationalize some of the discrepancies. We have also considered the influence of such phenomena on heat and mass transfer[82].

Figure 17 shows such comparisons, which rationalize the type of discrepancies shown in Figure 15. We were indeed happy that we were able to explain the anomalies in momentum transfer in slipping polymer solutions. We turned our attention to heat and mass transfer also[82].

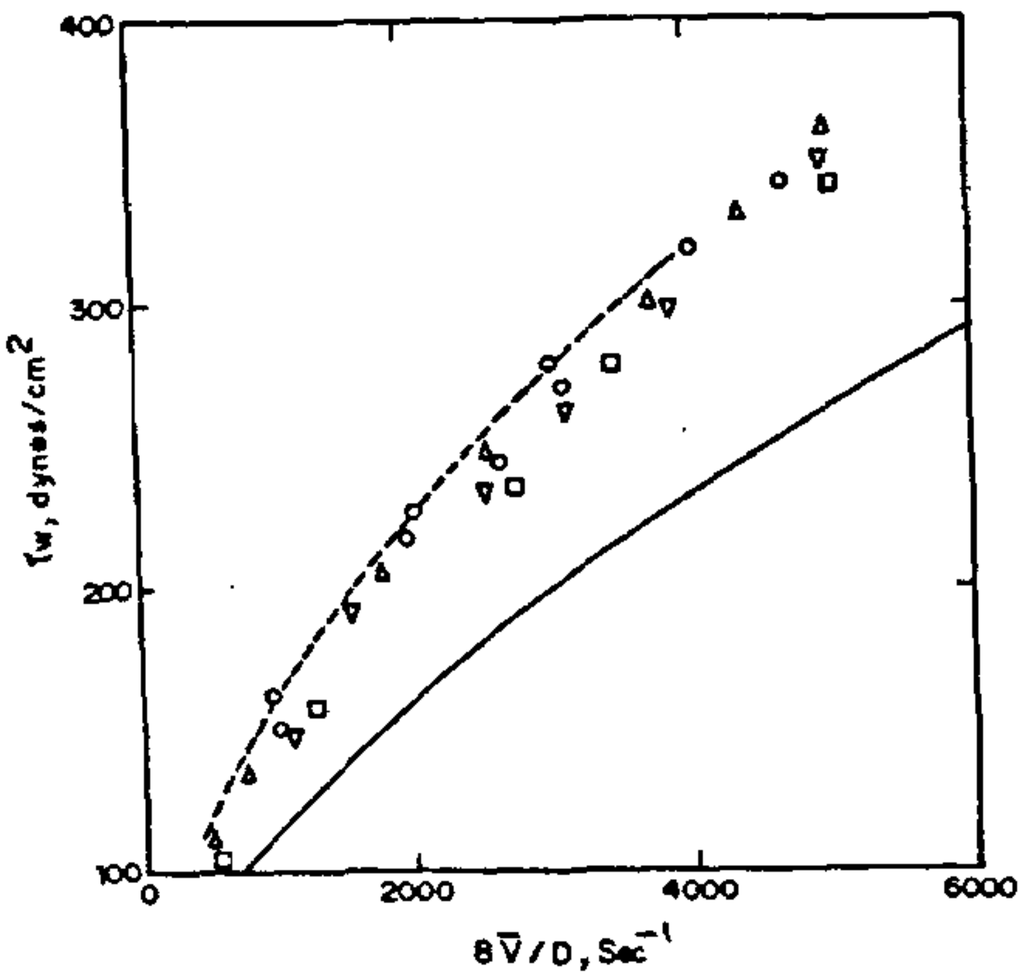

Figure 17. A comparison of the experimental data on a few dilute polymer solutions (0.25% separan AP-30) with conventional no-slip calculation (solid line) and Dutta and Mashelkar's[75] FDCF asymptotic computations (dashed line).

Our discussion so far has been biased by the work our school has done. It is also important to comment on other schools of thought in this area. One school of thought, based on hydrodynamic considerations, was propagated by Aubert and Tirrell[83]. The flexible polymer molecule in solution is modelled as a dumb-bell (two beads connected by linear, elastic spring, as shown in Figure 3) with the bead velocities given (by series expansion of the velocity field, **V**, about c the centre of the dumb-bell) as

$$\mathbf{V}_1 \sim \mathbf{V}_c(\mathbf{r}_c) - \frac{\mathbf{R}}{2}\cdot\nabla\mathbf{V} + \frac{1}{2}\frac{\mathbf{R}}{2}\frac{\mathbf{R}}{2}:\nabla\nabla\mathbf{V} \tag{34}$$

$$\mathbf{V}_2 \sim \mathbf{V}_c(\mathbf{r}_c) + \frac{\mathbf{R}}{2}\cdot\nabla\mathbf{V} + \frac{1}{2}\frac{\mathbf{R}}{2}\frac{\mathbf{R}}{2}:\nabla\nabla\mathbf{V}, \tag{35}$$

where **R** is the bead-to-bead vector. Now, the velocity of the centre of mass is obtained as

$$\dot{\mathbf{r}}_c = 0.5(\mathbf{V}_1 + \mathbf{V}_2) \approx \mathbf{V}_c(\mathbf{r}_c) + \frac{1}{8}\mathbf{RR}:\nabla\nabla\mathbf{V} \tag{36}$$

i.e. the molecule "migrates" with respect to the fluid with a velocity

$$\mathbf{V}^m = \dot{\mathbf{r}}_c - \mathbf{V}_c(\dot{\mathbf{r}}_c) = \frac{1}{8}\mathbf{RR}:\nabla\nabla\mathbf{V} \tag{37}$$

which results in a non-zero flux of the dumb-bells only in non-homogenous (i.e. position-dependent **V** flow field given by

$$\mathbf{J}^{nh} \sim C(\mathbf{r}_c)\,\mathbf{V}^m. \tag{38}$$

For example, in case of a Couette flow, this corresponds to a radial flux for the dumb-bell towards the inner cylinder, counterbalanced by the Brownian motion, given by

$$\mathbf{J}^{\text{Brown}} = -D\frac{\partial C}{\partial \mathbf{r}} \tag{39}$$

such that the equilibrium concentration profile is given by

$$\frac{dC}{dr} = -2C\frac{(\lambda\dot{\gamma})^2}{r}. \tag{40}$$

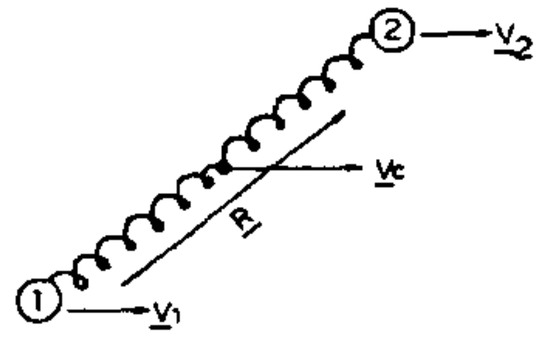

Figure 18. Bead velocities in an elastic dumb-bell model.

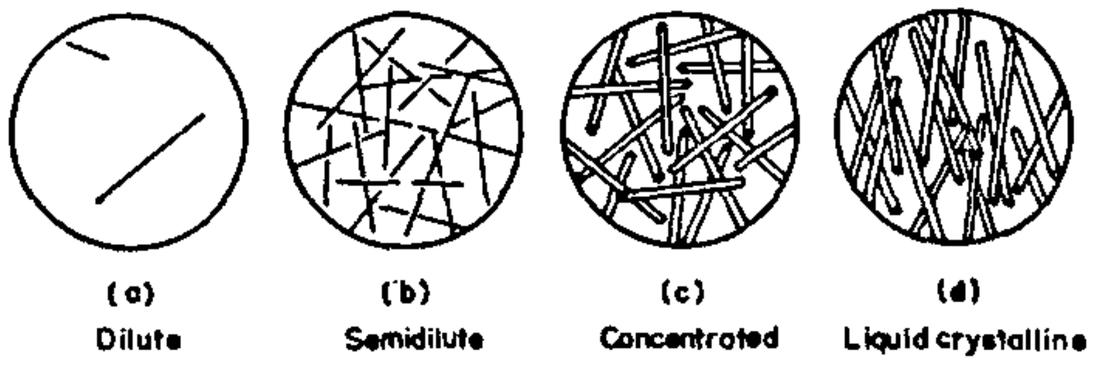

Figure 13. Concentration regimes for rigid rod-like molecules in solutions.

Aubert *et al.*[84] compared their theoretical results with experiments of Dill and Zimm[85] for concentration profile of DNA produced in a dilute solution between rotating concentric cones. The authors considered the quite good qualitative agreement to be rather 'fortuitous' in view of the involved parameter estimation, the chain model being infinitely extendable linearly elastic dumb-bell, neglect of hydrodynamic interaction between beads, assumption of dilute solution, and not reaching an equilibrium during the time of experiment. Subsequently, Brunn has considered many detailed aspects of the phenomenon in a series of papers [see, e.g. ref. 86, 87]. His essential conclusions are

- Radial migration cannot be predicted in rectilinear flow through channels, without incorporating the wall- effects, wherein the walls restrict the number of configurations available to the molecules near the walls, thereby causing a layer of depletion.
- Even if the wall exclusion mechanism is accounted for, the migration effect in tubes or channels is limited to distances of the order of molecular dimensions from the wall. This is not sufficient to explain the previously mentioned 'slip' effects. This is in contrast to the 'thermodynamic' theory mentioned before.
- The hydrodynamic theory cannot predict the migration to stagnant cavity, as mentioned earlier.
- In the case of circular flows (e.g. Couette flow), the hydrodynamic theory predicts migration radially inwards, as has been observed experimentally and discussed above; while the thermodynamic theory predicts radially outwards migration to the low shear region.

We conclude that in spite of the possible implications, no conclusive experimental study of this effect has been carried out, and also, no molecular mechanism consistent with the experimental observations is available. Some key issues in this case have been discussed by the MIT school[88]. Difficulties in concentration measurement in thin layers ($< 100\,\mu m$) of concentration depletion near the walls, and the problem of the residence time of the molecules in the flow field (e.g. capillary flows, wire withdrawal, etc.) being too small to permit equilibrium need special mention. While the effects may be substantial enough to have indirect implications, direct verification of the theories by concentration measurements in thin layers near wall is becoming a reality only recently. Aussere *et al.*'s[89] data obtained by evanescent fluorescence measurement techniques are noteworthy. In regard of the above difficulties, circular Couette flow fields offer a stronger promise, by way of as large as desired a residence time of the molecules in a controlled shear flow field. We have recently begun experiments with a polyacrylamide solution in a Couette flow field where a cavity of stagnant fluid is in contact with the flowing fluid at the outer wall.

Before closing, it is worthwhile commenting on the fact that we are beginning to look at solutions of rigid rod-like polymers which offer even more interesting behaviour in this regard. Let us first discuss the general important features of such polymers, and then discuss the important features of our theoretical developments in this regard.

Polymers like poly(*para*-phenylene terephthalamide) are extended in one direction along the aromatic back bone due to their rigidity and *para*-coupling, resulting in their rod-like structure. Besides, there are many examples of naturally occurring rodlike molecules. These include polypeptides like poly(γ-benzyl-L-glutamate), xanthan-polysaccharides, etc. and several other biological molecules. While segmental mobility of flexible molecules is high due to rapid bond rotations, in the case of rigid rod-like (RRL) molecules, the diffusion of the entire molecule must be cooperative and hence slow. Mobility of RRL molecules can be described in terms of three different diffusivities—translational diffusivity parallel to rod-axis, translational diffusivity perpendicular to rod-axis, and rotational diffusivity about the rod-centre.

The very strong molecular length (L) dependence of the rotational diffusivity ($D_r \sim L^{-9}$) and the vanishing translational diffusivity perpendicular to the rod-axis of such polymers in semidilute solutions (see Figure 19) are noteworthy, and are important as regards the polymer migration phenomena. We have analysed the problem in the framework of hydrodynamic theory concept. We have obtained results for a rigid dumb-bell (with the flexible spring replaced by a rigid rod) in a Couette flow. We have shown[90] that the above peculiarities of diffusivity of RRL molecules result in creation of large concentration gradients.

There are many fascinating aspects of the problem of migration that continue to open up, even in the case of flexible polymer molecules. One of the key points that may be missed is the question of molecular diffusion of macromolecules. As we have indicated earlier, molecular diffusion will try to bring the macromolecules closer to the stressed surface when entropic forces have moved

them away. It is only recently that it has been realized that molecular diffusivity of macromolecules does depend upon rate of shear. Recently we have done calculations[91,92] to provide a physical basis for the shear dependent molecular diffusivity in polymer solutions based on molecular models of polymer solutions. If one incorporates a shear rate-dependent diffusivity in the analysis then one finds that the level of concentration gradients that could be set up will be very considerably reduced. Mavrantzas and Beris[93], in their recent theoretical study of the wall effects on the rheology of dilute polymer solutions, have also commented on the role of anisotropic diffusion of polymer diffusion on migration. Thus Mansfield and Theodoron[94] study the diffusive motion of the polymer chains near a solid wall and show that the diffusivity in the direction perpendicular to the wall is several times less than that in the bulk. Such anisotropic and shear effects will certainly have to be incorporated in future developments.

One might wonder as to what are the implications of such macromolecular migrations in real practice. Well, they are rather profound and that is why we have been interested in these phenomena. Consider the case of secondary oil recovery in petroleum fields. There have been observations on polymer retention in stagnant zones[95] and one has not been able to explain these so far. This is probably directly linked to stress-induced migration.

The flow-induced concentration differences may relate to physiology also[96]. Consider the structure of endothelium layers in a typical wall, including the intercellular channels, void spaces and the cavioles, which are precursors to vesicules. As the arterial blood stream flows past into these structures, the macromolecular species in the flowing stream could diffuse into these wall cavities. If this is so then the predicted concentration gradients will influence the diffusional transport of these molecular species from the wall cavities into other parts of endothelium including the cells.

It has been argued that the free cholesterol ester and the cholesterol monohydrate in atherosclerotic plaque could be attributed to such concentration excesses. Janssen and Metzner[96] cite the evidence of some *in vitro* experiments, which show that the uptake of albumin by the arterial wall in the higher stress range varies with the square of shear stress, a dependence, which can be shown to arise from equation (31). The migration of some of the macromolecular compounds of blood towards a backwater region may be expected to lead to many interesting phenomena in view of the fact that we are dealing with very slow processes in physiology: possibly for some species having limited solubility, even a minor concentration excess might be quite significant.

We have earlier alluded to the problem of instabilities in polymer flows and specifically referred to the sharkskin effect. Chen and Joseph[97] tentatively invoke, as an explanation of sharkskin, the hypothesis that high stresses near the capillary wall could cause migration of polymer from the solid wall. Equivalently, low-molecular-weight components can become concentrated in a thin wall layer. They show that the stratification of elasticity accompanying such polymer migration phenomena can lead to short-wave hydrodynamic instabilities under some circumstances. These instabilities would presumably propagate to the die exit and create surface distortions.

There are perhaps other implications of the migration phenomena, that we have not even recognized. It is certain that this fascinating field will continue to attract the attention of the researchers in the coming decade.

Concluding remarks

In the foregoing, we have described some aspects of the fascinating behaviour of non-Newtonian fluids. The empirical approach to the description of such fluids has now given way to a more fundamental molecular modelling approach. We have given a bird's eye view of the recent advances of modelling in this area, commenting at the same time on the new frontiers of research that are opening up.

Further developments and refinements in molecular modelling will continue to be made. However, as an engineer, I find that even the existing knowledge base will find interesting applications as regards the elucidation of transport problems of direct interest to engineers. Let us take, as an example, the reptation model. Consider, for instance, the question of the prediction of the life time of a polymer particle that dissolves in a solvent. We have shown[98] that the interesting coupling between the cooperative diffusion of the physically entangled network during swelling as well as the reptation of the long chain molecules from the swollen polymer leads us to an interesting conclusion, namely that the life time of the dissolving particle will be independent of the particle size after a minimum size is reached. This is in sharp contrast to what is observed in ordinary materials, where finer the size, faster is the dissolution. The basic ideas of reptation have also been used very effectively in predicting the welding behaviour of two polymers that are brought together. Recently we have used[99] such methods to show the difficulties one will encounter in welding of rigid rod-like polymers, an observation, which is of great importance in the processing of melt processible liquid crystalline materials. Due to want of space we have not alluded to many of these interesting findings. But it is important to remark that an

engineer's familiarity with these basic concepts will help him enormously in analysing and designing systems with insight and perception.

In this article, we specifically considered three topics related to instabilities in polymer fluid flows, flows past submerged objects and stress-induced demixing of polymeric fluids. The idea was not only to bring out the progress that has been made and the problems that still remain unresolved, but also the difficulties one faces in even the conceptual handling of some of the problems.

As we have pointed out, although great deal of progress has been made in numerical modelling of complex flows of non-Newtonian fluids, yet we find that an apparently simple problem of the flow of a very dilute polymer solution of few parts per million of polymer past a cylinder has remained unresolved after 25 years of the discovery of the velocity independent heat and mass transport coefficient behaviour! How should engineers proceed then? By using heuristic arguments and deep physical insight, engineers will have to find their way through. The superb engineering analysis[100,101] on drop break-up and coalescence in turbulently stirred dispersions of non-Newtonian fluids made by Prof. Kumar and Prof. Gandhi of the Indian Institute of Science is a brilliant testimony to the way engineers find solutions to difficult problems, even when they have to deal with such complex flows!

What about the future? Clearly a more detailed understanding at the microscopic as well as macroscopic levels will be needed to understand many complex phenomena associated with many structurally complex materials. One already sees a great deal of progress in this direction. Sophisticated flow visualization experiments, numerical experiments (with powerful supercomputers), as well as *in situ* experiments on studying the dynamics of motion of polymers at a molecular level (see, for example, the recent study by Akatani *et al.*[102] on solid state NMR of a polymer melt under shear) are certainly going to lead the way in our understanding the beauty of these admittedly bizarre, but certainly most fascinating fluids, which exhibit non-Newtonian behaviour.

1. Bird, R. B., Curtiss, C. F., Armstrong, R. C. and Hassager, O., *Dynamics of Polymeric Liquids, vol. 1 (Fluid Mechanics) and vol. 2 (Kinetic Theory)*, Wiley, New York, 1987.
2. Crochet, M. J., Davies, A. R. and Walters, K., *Numerical Simulation of Non-Newtonian Flow*, Elsevier, Amsterdam, 1984.
3. Barnes, H. A., Hutton, J. F. and Walters, K., *An Introduction to Rheology*, Elsevier, Amsterdam, 1989.
4. Ferry, J. D., *Viscoelastic Properties of Polymers*, Wiley, New York, 1980, 3rd edn.
5. Mashelkar, R. A., Kale, D. D., Kelkar, J. V. and Ulbrecht, J., *Chem. Eng Sci.*, 1972, **27**, 973.
6. Mashelkar, R. A., in *Rheology 1*, (eds. Astarita, G., Marrucci, G. and Nicolais, L.), Plenum, New York, 1980, p. 219.
7. Noll, W., *Arch. Ration. Mech. Anal.*, 1958, **2**, 197.
8. Green, M. S. and Tobolsky, A. V., *J. Chem. Phys.*, 1946, **14**, 80.
9. Lodge, A. S., *Rheol. Acta*, 1968, **7**, 379.
10. Flory, P. J., *Statistical Mechanics of Chain Molecules*, Interscience (Wileys), New York, 1969.
11. Marrucci, G., in *Transport Phenomena in Polymeric Systems* (eds. Mashelkar, R. A., Majumdar, A. S. and Kamal, R.,), vol. 6, Ellis Horwood, Chichester, 1989.
12. de Gennes, P. G., *Scaling Concepts in Polymer Physics*, Cornell University, Ithaca, New York, 1979.
13. Doi, M. and Edwards, S. F., *The Theory of Polymer Dynamics*, Clarendon Press, Oxford,1986.
14. Edwards, S. F., *Proc. Phys. Soc.*, 1967, **92**, 9.
15. Osaki, K., Fukuda, M. and Kurata, M., *J. Polym. Sci.*, 1957, **13**, 775.
16. Larson, R. G., *Rheol. Acta*, 1992, **31**, 213.
17. Boger, D. V., Hur, D. V. and Binnington, R. J., *J. Non-Newtonian Fluid Mech.*, 1986, **20**, 31.
18. Raiford, W. P., Quinzani, L. M., Coates, P. J., Armstrong, R. C. and Brown, R. A., *J. Non-Newtonian Fluid Mech.*, 1989, **32**, 39.
19. Giesekus, H., *Rheol. Acta*, 1968, **7**, 127.
20. Cable, P. J. and Boger, D. V., *AIChE J*, 1978, **24**, 869.
21. Cable, P. J. and Boger, D. V., *AIChE J*, 1978, **24**, 882.
22. Cable, P. J. and Boger, D. V., *AIChE J*, 1979, **25**, 152.
23. Nguyen, H. and Boger, D. V., *J. Non-Newtonian Fluid Mech.*, 1979, **5**, 353.
24. McKinley, G. H., Raiford, W. P., Brown, R. A. and Armstrong, R. C., *J. Fluid Mech.*, 1991, **223**, 411.
25. Lawler, J. V., Muller, S. J., Brown, R. A. and Armstrong, R. C., *J. Non-Newtonian Fluid Mech.*, 1986, **20**, 51.
26. Tordella, J. P., in *Rheology* (ed. Eirich, F. R.), Academic Press, New York, vol. 5, 1969.
27. Petrie, C. J. S. and Denn, M. M., *AIChE J*, 1976, **22**, 209.
28. Ramamurthy, A. V., *J. Rheol.*, 1986, **30**, 337.
29. Piau, J. M., Kissi, N. El., and Themblay, B., *J. Non-Newtonian Fluid Mech.*, 1990, **34**, 145.
30. Benbow, J. J. and Lamb, P., *SPE Trans.*, 1963, **3**, 7.
31. Kissi, N. El. and Piau, J. M., *J. Non-Newtonian Fluid Mech.*, 1990, **37**, 55.
32. Kalika, D. S. and Denn, M. M., *J. Rheol.*, 1987, **31**, 815.
33. Denn, M. M., *Annu. Rev. Fluid Mech.*, 1990, **22**, 13.
34. Moynihan, R. H., Baird, D. G. and Ramanathan, R., *J. Non-Newtonian Fluid Mech.*, 1990, **36**, 255.
35. Pearson, J. R. A. and Petrie, C. J. S., in *Polymer Systems. Deformation and Flow* (eds. Wetton, R. E and Whorlow, R. W.), McMillan, London, 1968.
36. Renardy, M., *J. Non-Newtonian Fluid Mech.*, 1990, **35**, 73.
37. Hill, D. A., Hasegawa, T. and Denn, M. M., *J. Rheol.*, 1990, **34**, 891.
38. Huseby, T. W., *J. Rheol.*, 1966, **10**, 181.
39. Schowalter, W. R., *J. Non-Newtonian Fluid Mech.*, 1988, **29**, 25.
40. McLeish, T. C. B. and Ball, R. C., *J. Polym. Sci. Polym. Phys.*, 1986, **24**, 1735.
41. Paul, D. R. and Sonthern, J. H., *J. Appl. Polym. Sci.*, 1975, **19**, 3375.
42. Doi, M. and Edwards, S. F., *J. Chem. Soc. Faraday Trans. II*, 1979, **75**, 32.
43. Deiber, J. A. and Schowalter, W. R., *J. Non-Newtonian Fluid Mech.*, 1991, **40**, 141.
44. Vinogrodov, G. V., Ya Malkin, A., Yankovsun, Yu. G., Borisenmova, E. K., Yarlykov, B. V. and Berezhnaya, G. V., *J. Polym. Sci. (A 2)*, 1972, **10**, 1061
45. Vinogrodov, G. V., *Rheol. Acta*, 1975, **14**, 942.
46. Kenuings, R., *J. Non-Newtonian Fluid Mech.*, 1986, **20**, 209
47. Coates, P. J., Armstrong, R. C. and Brown, R. A., *J. Non-Newtonian Fluid Mech.*, in press.
48. Acharya, A., Mashelkar, R. A. and Ulbrecht, J., *Rheol. Acta*, 1976, **15**, 454.

49. Zheng, R., Phan-Thien, N. and Tanner, R. I., *J. Non-Newtonian Fluid Mech.*, 1990, **36**, 27.
50. Acharya, A., Mashelkar, R. A. and Ulbrecht, J., *Rheol. Acta*, 1976, **15**, 471.
51. Ambeskar, V. D., *Transport Phenomena in Polymeric Media*, Ph D Thesis, University of Bombay, Bombay, 1990.
52. Ambeskar, V. D. and Mashelkar, R. A., *Rheol. Acta*, 1990, **29**, 182
53. Riddle, M. J., Narvaez, C. and Bird, R. B., *J. Non-Newtonian Fluid Mech.*, 1977, **2**, 23.
54. Bhavaraju, S., Mashelkar, R. A. and Blanch, H. W., *AIChE J.*, 1978, **24**, 1063.
55. Bhavaraju, S., Mashelkar, R. A. and Blanch, H. W., *AIChE J.*, 1978, **24**, 1070.
56. Acharya, A., Mashelkar, R. A. and Ulbrecht, J., *Chem. Eng. Sci.*, 1977, **32**, 863.
57. Astarita, G. and Apuzzo, G., *AIChE J.*, 1965, **11**, 815.
58. Bond, W. N. and Newton, D. A., *Philos. Mag*, 1924, **5**, 793.
59. Acharya, A., Mashelkar, R. A. and Ulbrecht, J., *Can. J. Chem. Eng.*, 1978, **56**, 19.
60. Hassager, O., *Nature*, 1979, **279**, 5712.
61. James, D. F. and Acosta, A. J., *J. Fluid. Mech.*, 1970, **42**, 269.
62. James, D. F. and Gupta, O. P., *Chem. Eng. Progr.*, 1971, **67**, 62.
63. Metzner, A. B. and Astarita, G., *AIChE J.*, 1967, **13**, 550.
64. Denn, M. M. and Marrucci, G., *AIChE J.*, 1971, **17**, 101.
65. Ultmann, J. S. and Denn, M. M., *Trans. Soc. Rheol.*, 1970, **14**, 307.
66. Yoo, J. Y. and Joseph, D. D., *J. Non-Newtonian Fluid Mech.*, 1985, **19**, 15.
67. Joseph, D. D., Renardy, M. and Sant, J. C., *Arch. Ration Mech. Anal.*, 1985, **87**, 213.
68. Tanner, R. I., *Z. Angew. Math. Phys.*, 1962, **13**, 573.
69. Mashelkar, R. A. and Marrucci, G., *Rheol. Acta*, 1980, **19**, 426.
70. Piau, J. M., *C. R. Acad. Sci. Paris*, 1974, **B278**, 493.
71. Ambari, A., Deslonis, C. and Tribollet, B., *Chem. Eng. Commun.*, 1984, **29**, 63.
72. Metzner, A. B., in *Improved Oil Recovery by Surfactant and Polymer Flooding*, (eds. Shah, D. O. and Schechter, R. S), Academic Press, New York, 1977.
73. Metzner, A. B., Cohen, Y. and Ranger Natalie, C., *J. Non-Newtonian Fluid Mech.*, 1979, **5**, 449.
74. Tirrell, M. and Malone, M. F., *J. Polym. Sci.*, 1977, **15**, 1569.
75. Dutta, A. and Mashelkar, R. A., *J. Non-Newtonian Fluid Mech.*, 1984, **16**, 279.
76. Gutfinger, C. and Tallmadge, J. A., *AIChE J.*, 1965, **11**, 403.
77. Mashelkar, R. A. and Dutta, A., *Chem. Eng. Sci.*, 1982, **37**, 969.
78. Dutta, A. and Mashelkar, R. A., *Chem. Eng. Commun.*, 1985, **39**, 277.
79. Dutta, A. and Mashelkar, R. A., *AIChE J.*, 1983, **29**, 519.
80. Dutta, A. and Mashelkar, R. A., *Rheol. Acta*, 1983, **22**, 455.
81. Dutta, A., Ravetkar, D. D. and Mashelkar, R. A., *Chem. Eng. Commun.*, 1987, **53**, 161.
82. Dutta, A. and Mashelkar, R. A., *Chem. Eng. Commun.*, 1985, **33**, 181.
83. Aubert, J. H. and Tirrell, M., *J. Chem. Phys.*, 1980, **72**, 2694.
84. Aubert, J. H., Prager, S. and Tirrell, M., 1980, **73**, 4103.
85. Dill, K. O. and Zimm, B. H., *Nucleic Acids Res.*, 1979, **7**, 735.
86. Brunn, P. O., *J. Rheol*, 1985, **29**, 859.
87. Brunn, P. O. and Grisafi, S., *Rheol. Acta*, 1987, **26**, 211.
88. Bhave, A., Armstrong, R. C. and Brown, R. A., *J. Chem. Phys.*, 1991, **95**, 2988.
89. Aussere, D., Edwards, J., Lecowatier, J., Herwet, H. and Rondelez, F., *Europhys. Lett.*, 1991, **14**, 33.
90. Agarwal, U. S. and Mashelkar, R. A., manuscript in preparation.
91. Ravi Prakash, J. and Mashelkar, R. A., *J. Chem. Phys.*, 1991, **95**, 3743.
92. Ravi Prakash, J. and Mashelkar, R. A., *J. Rheol.*, 1992, **36**, 789.
93. Mavrantzas, V. G. and Beris, A. N., *J. Rheol.*, 1992, **36**, 175.
94. Mansfield, K. V. and Theodoron, D. N., *Macromolecules*, 1989, **22**, 3143.
95. Maerker, J. M, *J. Pet. Tech.*, 1973, **25**, 1307.
96. Janssen, L. P. B. M. and Metzner, A. B., *Phys. Med. Biol.*, 1980, **25**, 343.
97. Chen, K. and Joseph, D. D., *J. Non-Newtonian Fluid Mech.*, 1992, in press.
98. Premnath, V., Kulkarni, M. G., Mandhre, A. B. and Mashelkar, R. A., manuscript in preparation.
99. Agarwal, U. S. and Mashelkar, R. A., *Macromolecules*, 1992, (in press).
100. Koshy, A., Kumar, R. and Gandhi, K. S, *Chem. Eng. Sci.*, 1989, **44**, 2113.
101. Koshy, A., Das, T. R., Kumar, R. and Gandhi, K. S., *Chem. Eng. Sci.*, 1988, **43**, 2625.
102. Akatani, A. I., Poliks, M. D. and Samulski, E. T., *Macromolecules*, 1990, **29**, 2686.